J|A|C|S
ARTICLES
Published on Web 08/28/2003

Identity Proton-Transfer Reactions from C−H, N−H, and O−H Acids. An ab Initio, DFT, and CPCM-B3LYP Aqueous Solvent Model Study

James R. Keeffe,*,† Scott Gronert,*,† Michael E. Colvin,‡,§ and Ngoc L. Tran†,‡

Contribution from the Department of Chemistry and Biochemistry, San Francisco State University, 1600 Holloway Avenue, San Francisco, California 94132, Computational Biology Group and Biotechnology Research Program, Lawrence Livermore National Laboratory, Scientific Computing Department, Mailstop L-448, Livermore, California 94550, and Department of Chemistry, University of California, Merced, California 95344

Received April 16, 2003; E-mail: sgronert@sfsu.edu

Abstract: Identity proton-transfer reactions between 21 acids, Y−X−H, and their conjugate bases, $^{-}$X−Y, were studied according to the reaction scheme, Y−X−H + $^{-}$X−Y → (Y−X−H····$^{-}$X−Y)$_{cx}$ → [Y−X···H···X−Y]$_{ts}$ → (Y−X^{-}····H−X−Y)$_{cx}$ → Y−X^{-} + H−X−Y, where cx indicates an ion−molecule complex and ts indicates the proton-transfer transition state. All species were optimized at the MP2/6-311+G** level, and these geometries were used for single-point calculations by other methods: coupled-cluster, DFT (gas phase), and a polarizable continuum aqueous solvent model (COSMO). All methods gave enthalpies of deprotonation which correlate well with experimental measurements of ΔH_{ACID} (gas) or pK_a (aq). Calculated gas-phase enthalpies of deprotonation (ΔH_{ACID}) and enthalpies of activation ($\Delta H^{\ddagger}$) are poorly correlated except for small, carefully selected sets. This result stands in contrast to the many aqueous phase Brönsted correlations of kinetic and equilibrium acid strength. On the other hand, gas-phase enthalpies of complexation and $\Delta H^{\ddagger}$ are well correlated, indicating that factors which stabilize the transition state are at work in the bimolecular ion−molecule complex although to a smaller degree. We infer that intermoiety electrostatic and other interactions, similar within the complex and the transition state, but absent in the separated reactants (products), cause the lack of correlation between ΔH_{ACID} and the other two quantities. Such differences are strongly attenuated in water because reactants and products do interact with polar/polarizable matter (the solvent) if not with each other. Charge distributions (NPA) were computed, allowing calculation of Bernasconi's "transition state imbalance parameter". Such measures provide intuitively satisfactory trends, but only if the reaction termini, X, are kept the same. As X is made more electronegative, the magnitude of the apparent imbalance increases, a result of greater negative charge on X in the transition state. This result gives additional support for the importance of the ion-triplet structure, [YX^{-}···H^{+}···$^{-}$XY], to the stability of the transition state. Additional qualitative support for this conclusion is provided by the inverse relationship between the activation barrier and the charge on the in-flight hydrogen in the transition state, and by the dominance of polar over resonance substituent effects on the stability of the transition state. Calculations also show that the "nitroalkane anomaly", well established in solution, does not exist in the gas phase. The COSMO model partly reproduces this anomaly and performs adequately except when strong, specific intermolecular forces such as hydrogen bonding between solvent and anions are important.

Introduction

The enormous importance of acid- and base-catalyzed reactions in chemistry and biochemistry has made the study of proton transfer one of constant relevance. Experimental work on solution-phase reactions has continued for over a century,[1−8] giving rise to a large amount of knowledge about reaction mechanisms and relationships between molecular structure and chemical reactivity. More recently, gas-phase measurements of rate and equilibrium constants for proton-transfer reactions have become numerous,[9] highlighting both similarities and differences

† San Francisco State University.
‡ Lawrence Livermore National Laboratory.
§ U.C. Merced.

(1) (a) Lapworth, A.; Hann, A. C. O. *J. Chem. Soc.* **1902**, 1508. (b) Lapworth, A. *J. Chem. Soc.* **1904**, 30.
(2) (a) Bell, R. P. *Acid−Base Catalysis*; Oxford University Press: London, 1941. (b) Bell, R. P. *The Proton in Chemistry*, 2nd ed.; Cornell University Press: Ithaca, NY, 1973.
(3) Eigen, M. *Angew. Chem., Int. Ed. Engl.* **1964**, *3*, 1.
(4) Bruice, T. C.; Benkovic, S. J. *Bioorganic Mechanisms*; Benjamin: New York, 1966.
(5) Jencks, W. P. *Catalysis in Chemistry and Enzymology*; McGraw-Hill: New York, 1969.
(6) Caldin, E. F., Gold, V., Eds.; *Proton-Transfer Reactions*; Chapman and Hall: London, 1975.
(7) Stewart, R. *The Proton−Applications to Organic Chemistry*; Academic Press: San Diego, 1985.
(8) Keeffe, J. R.; Kresge, A. J. In *Investigation of Rates and Mechanisms of Reactions*, 4th ed.; Bernasconi, C. F., Ed.; Wiley-Interscience: New York, 1986; Part 1, Chapter XI.

10.1021/ja0356683 CCC: $25.00

between solution-phase and innate, medium-free reactivity. Additionally, a host of pertinent theoretical and computational studies have also been reported.[10−13]

It has long been known that some aqueous-phase acid−base combinations result in much faster proton transfers than other combinations, even when thermodynamic biases are accounted for. This knowledge was put on a quantitative basis by Eigen and co-workers.[3] So-called "Eigen-normal" acids and bases undergo proton transfer in the exoergic direction at encounter controlled rates, or nearly so.[2b,3] Notable among the slower acids and bases are those for which proton transfer occurs to or from a carbon atom. For example, phenol ($pK_a = 10.0$) reacts with hydroxide ions in aqueous solution approximately 4×10^5 faster than does 2,4-pentanedione ($pK_a = 9.0$)[3] and 5×10^8 faster than does nitromethane ($pK_a = 10.2$).[14] As may be inferred from the difference in reactivity between 2,4-pentanedione and nitromethane, C−H acids themselves do not comprise a homogeneous group. Rather, they too disperse into several subgroups when correlations between log k and log K_a are made.[15] Apparently, the factors which stabilize the conjugate base relative to the conjugate acid form are expressed much differently in the transition states of the various groups and subgroups: better for the faster acids and poorer for the slower acids.

Small rate reductions for C−H acids have been observed in the gas phase as well. Brauman et al. have determined that proton transfer from ethanol to methoxide ion is 16 times faster than proton transfer from toluene to allyl anion despite the latter reaction having a free energy of reaction advantage of about 6 kcal/mol.[9a] Moreover, the endoergic reaction of ethoxide with methanol is as fast as the ergoneutral reaction between toluene and benzyl anion despite an ca. 3.5 kcal/mol thermodynamic disadvantage.[9c]

Additional information and some insight come from structure−reactivity relationships between rates and equilibria for C−H acids. One classic example is the contrast between the relative aqueous pK_a values of nitromethane, nitroethane, and 2-nitropropane and their rates of deprotonation. The acidities of these nitroalkanes increase in the order given, but the rates of deprotonation by OH^-/H_2O follow the opposite order.[16] Another example was the finding that, although Brönsted β-values for the aqueous-phase deprotonation of a given arylnitromethane by Eigen-normal bases are unremarkable ($\beta = d \log k_B/d\ pK_{BH} = 0.5-0.6$), the Brönsted α values ($\alpha = -d \log k_A/d\ pK_A$) obtained by varying the acidity of the arylnitroalkanes toward a given base are "anomalous", being greater than 1.0.[17,18] Such a result indicates that the effect of the structural change in the C−H acid (*m*- and *p*-substituents were varied) is greater on the proton-transfer transition state than on the fully formed conjugate base product. These results stand in contrast to proton transfer between normal acids and bases which exhibit equal or nearly equal α and β values lying between 0 and 1.[3]

Explanations for such behavior have focused on contrasts between the structure of the anionic product and the imagined structure of the ts. Conjugate bases of the most acidic C−H acids are typically stabilized by resonance delocalization or relocation of the negative charge from the carbon at which proton loss occurred to remote, more electronegative atoms. This charge shift takes place with concomitant changes in one or more bond lengths as shown in the two examples below. At the transition state, only a fraction of the charge has been transferred from, say, an anionic base to the carbon acid moiety.

$$O_2N-CH_3 \rightarrow {}^-O_2N{=}CH_2$$

$$O{=}CH-CH_3 \rightarrow {}^-O-CH{=}CH_2$$

One may propose, as did Kresge, that only a fraction of this fraction has been relocated at the ts; hence the features stabilizing the conjugate base are but poorly developed at the ts.[16] The transition state may be said to be imbalanced with respect to the degree of proton transfer, on one hand, and other changes (e.g., bond lengths and orders, charge, and solvent shifts) on the other. The energetic consequences have been analyzed both from the electrostatic viewpoint[19] and as a manifestation of the "Principle of Least Nuclear Motion".[20] Bernasconi has broadened and formalized the concept and the questions raised by such behavior under the "Principle of Nonperfect Synchronization".[16c,21]

A prediction which follows from this interpretation is that the large disparity between the α and β values measured for the arylnitromethane reactions cited above is largely due to strong hydrogen-bonding solvation of the two negative oxygens

(9) (a) Brauman, J. I.; Lieder, C. A.; White, M. J. *J. Am. Chem. Soc.* **1973**, *95*, 927. (b) Brauman, J. I.; Farneth, W E. *J. Am. Chem. Soc.* **1976**, *98*, 7891. (c) Han, C.-C.; Brauman, J. I. *J. Am. Chem. Soc.* **1989**, *111*, 6491. (d) Bohme, D. K.; Rakshit, A. B.; Mackay, G. I. *J. Am. Chem. Soc.* **1982**, *104*, 1100. (e) Moylan, C. R.; Brauman, J. I. *Annu. Rev. Phys. Chem.* **1983**, *34*, 187. (f) Bowers, M. T., Ed. *Gas-Phase Ion Chemistry*; Academic Press: New York, 1979. (g) Taft, R. W.; Topsom, R. D. *Prog. Phys. Org. Chem.* **1987**, *16*, 1 and references therein. (h) Brickhouse, M. D.; Squires, R. R. *J. Am. Chem. Soc.* **1988**, *110*, 2706. (i) Dodd, J. A.; Baer, S.; Moylan, C. R.; Brauman, J. I. *J. Am. Chem. Soc.* **1991**, *113*, 5942. (j) Yamataka, H.; Mustanir; Mishima, M. *J. Am. Chem. Soc.* **1999**, *121*, 10223. (k) Bartmess, J. E. In *NIST Standard Reference Database Number 69*; Mallard, W. G., Linstrom, P. J., Eds.; National Institute of Standards and Technology (http://webbook.nist.gov): Gaithersburg, MD, 1999. (l) Tran, N. L.; Colvin, M. E. *J. Mol. Struct. (THEOCHEM)* **2000**, *532*, 127.

(10) (a) Scheiner, S. *Acc. Chem. Res.* **1985**, *18*, 174; **1994**, *27*, 402. (b) Wolfe, S.; Hoz, S.; Kim, C.-K.; Yang, K. *J. Am. Chem. Soc.* **1990**, *112*, 4186. (c) Gronert, S. *Organometallics* **1993**, *12*, 3805. (d) Gronert, S. *J. Am. Chem. Soc.* **1993**, *115*, 10258. (e) Reference 9h.

(11) (a) Bernasconi, C. F.; Wenzel, P. J. *J. Am. Chem. Soc.* **1994**, *116*, 5405. (b) Bernasconi, C. F.; Wenzel, P. J.; Keeffe, J. R.; Gronert, S *J. Am. Chem. Soc.* **1997**, *119*, 4008. (c) Bernasconi, C. F.; Wenzel, P. J. *J. Am. Chem. Soc.* **2001**, *123*, 7146. (d) Bernasconi, C. F.; Wenzel, P. J. *J. Org. Chem.* **2001**, *66*, 968.

(12) (a) Pross, A.; Shaik, S. *J. Am. Chem. Soc.* **1982**, *104*, 1129. (b) Saunders, W. H., Jr. *J. Am. Chem. Soc.* **1994**, *116*, 5400. (c) Saunders, W. H., Jr.; Van Verth, J. E. *J. Org. Chem.* **1995**, *60*, 3452. (d) Van Verth, J. E.; Saunders, W. H., Jr.; Kermis, T. W. *Can. J. Chem.* **1998**, *76*, 821. (e) Van Verth, J. E.; Saunders, W. H., Jr. *Can. J. Chem.* **1999**, *77*, 810. (f) Harris, N.; Wei, W.; Saunders, W. H., Jr.; Shaik, S. *J. Am. Chem. Soc.* **2000**, *122*, 6754. (g) Wei, W.; Shaik, S.; Saunders, W. H., Jr. *J. Phys. Chem. A* **2002**, *106*, 11616.

(13) See refs 10a, 11c, and 11d for other pertinent references.

(14) Bell, R. P.; Goodall, D. M. *Proc. R. Soc. A* **1966**, *294*, 273.

(15) Davies, M. H.; Robinson, B. H.; Keeffe, J. R. *Annu. Rep. A* **1973**, 123.

(16) (a) Kresge, A. J. *Chem. Soc. Rev.* **1973**, *2*, 475. (b) Kresge, A. J. *Can. J. Chem.* **1974**, *52*, 1897 and references therein. (c) See also: Albery, W. J.; Bernasconi, C. F.; Kresge, A. J. *J. Phys. Org. Chem.* **1988**, *1*, 29.

(17) Fukuyama, M.; Flanagan, P. W. K.; Williams, F. T., Jr.; Frainier, L.; Miller, S. A.; Schecter, H. *J. Am. Chem. Soc.* **1970**, *92*, 4689.

(18) (a) Bordwell, F. G.; Boyle, W. J., Jr. *J. Am. Chem. Soc.* **1971**, *93*, 511. (b) Bordwell, F. G.; Boyle, W. J., Jr. *J. Am. Chem. Soc.* **1972**, *94*, 3907. Brönsted coefficients for proton-transfer events almost always lie between the limits ($0 < \alpha$ or $\beta < 1$). They are commonly taken as rough measures of the progress of the transfer at the transition state: α as reported by a set of acids and β when reported by a set of bases. It is recognized that the approximation can be a crude one. Among other reasons, the transition state of a bimolecular reaction step experiences interactions which do not exist in the separated reactants or products. See also ref 8, sections 4 and 7.2.1, ref 12a, and ref 16b.

(19) Reference 2b, Chapter 10. See also ref 16b.

(20) Hine, J. *Adv. Phys. Org. Chem.* **1977**, *15*, 1.

(21) (a) Bernasconi, C. F. *Acc. Chem. Res.* **1987**, *20*, 301. (b) Bernasconi, C. F. *Acc. Chem. Res.* **1992**, *25*, 9. (c) Bernasconi, C. F. *Adv. Phys. Org. Chem.* **1992**, *27*, 119.

in the nitronate product structure. This stabilizes the nitronate, enhancing the acidity of the nitroalkane, but the effect is not well developed at the transition state because of the lag in charge shift. If true, the difference between α and β should be smaller in solvents which are not H-bonding donors. Indeed, experiments in several solvents have produced the following differences ($\alpha - \beta$): For water[18] ($1.54 - 0.55 = 1.0$; for methanol[22c] ($1.31 - 0.50 = 0.8$; for DMSO[22a,b] ($0.92 - 0.49 = 0.4$; and for acetonitrile[22d] ($0.79 - 0.56 = 0.3$. The two parameters do not become equal, but their difference is reduced from almost 1.0 in water to 0.3 in acetonitrile. Additionally, the sluggishness at which arylnitromethanes are deprotonated in water is not so evident in other solvents. In DMSO, for example, at a given value of K_{eq}, rates average about 10^5 faster than those in water.[22a,b]

How might "transition state imbalance" (TSI) manifest itself in a quantitative or semiquantitave way? As implied above, one indicator might be the fractional changes which have occurred in bond lengths at the ts. This geometric indicator would take advantage of well-known correlations between bond order and bond length.[23] Another indicator could be fractional progress in charge shifts which have taken place at atoms or groups of atoms at the ts. A closely related issue is whether TSI exists in the gas phase, and, if so, what are its kinetic consequences? Experimentally, these questions are difficult to address, but computational explorations can be made.[10−12]

A useful approach is to study "identity" proton transfers, thereby canceling any thermodynamic bias given to the activation barrier. The result is termed an "intrinsic barrier" for the

$$Y{-}X{-}H + {}^{-}X{-}Y \rightarrow [ts]^{\ddagger} \rightarrow Y{-}X^{-} + H{-}X{-}Y \quad (1)$$

reaction. Saunders, Shaik, and co-workers have used both ab initio molecular orbital calculations and valence bond calculations to investigate the reactant and transition state structure in carbon-to-carbon (X = C),[12b,c,e] nitrogen-to-nitrogen (X = N),[12d] and oxygen-to-oxygen (X = O)[12e] proton transfers in eq 1. Bernasconi et al. have employed high level molecular orbital and DFT computations to do the same (X = C), and to quantitate imbalance according to the extent of charge relocation which has occurred when the acid reaches the transition state, then the conjugate base.[11] Important conclusions from these studies include the following: (1) TSI exists in the gas phase (although it may be exalted in solution as discussed above); (2) TSI does not necessarily increase activation barriers in the gas phase, in contrast to the situation in solution; (3) this is a consequence of the strong stabilization of the transition state especially by polar but also by polarizability effects of substituents which outweigh smaller barrier-raising resonance effects. In aqueous solution, strong solvation of the conjugate base anion stabilizes the reactant/product state more than the ts; (4) reaction via an imbalanced transition state, contrary to what intuition might predict, indeed represents the lowest energy pathway for gas-phase proton transfer. This is so because concentration of charge on the atoms represented by X enhances electrostatic or H-bonding stabilization of the transition state, whereas relocation of this charge and the concomitant geometry changes reduce this effect. This conclusion may be visualized by stating that valence bond resonance structure **1b**, an ion triplet, makes an important contribution to the ts structure, a contribution which would be diminished by charge delocalization.[24]

$$[Y{-}C{-}H\cdots{}^{-}C{-}Y \leftrightarrow \underset{\textbf{1a}}{Y{-}C^{-}\ H^{+}\ {}^{-}C{-}Y} \leftrightarrow \underset{\textbf{1b}}{} \qquad Y{-}C^{-}\cdots H{-}C{-}Y]^{\ddagger}$$
$$\textbf{1c}$$

In the present study, we have examined identity proton-transfer reactions defined as eq 2, where cx indicates an ion−molecule complex and ts indicates the transition state. The atoms, X, between which the proton is transferred are sp^3, sp^2,

$$Y{-}X{-}H + {}^{-}X{-}Y \rightarrow (Y{-}X{-}H\cdots{}^{-}X{-}Y)_{cx} \rightarrow [Y{-}X\cdots H\cdots X{-}Y]_{ts} \rightarrow (Y{-}X^{-}\cdots H{-}X{-}Y)_{cx} \rightarrow Y{-}X^{-} + H{-}X{-}Y \quad (2)$$

and sp hybridized carbon as well as oxygen, nitrogen, and silicon. Groups Y are various hydrocarbon groups or common acid strengthening groups such as nitro, carbonyl, cyano, and trifluoromethyl. All structures were optimized at the MP2/6-311+G** level. These structures were used for single-point energy and NPA charge determinations using DFT and coupled-cluster methods. We will address the relationships between gas-phase enthalpies of deprotonation, complexation, and activation as well as the utility of charge-based transition state imbalance parameters. Additionally, the effects of aqueous solvation were modeled using a polarizable continuum method, CPCM,[25] coupled to DFT.

Methods

All structures were built and optimized at the HF/3-21 or HF/6-31G* level using the MacSpartan Plus software package.[26] Conformational preferences were established at these levels, before completing the geometry optimizations at the HF/6-311+G** and MP2/6-311+G** levels using the Gaussian 94 or Gaussian 98 quantum mechanical packages.[27,28] Frequencies and zero-point vibrational energies were calculated at HF/6-311+G** at San Francisco State University, and then (in all but a few cases) at the MP2/6-311+G** level at Lawrence Livermore National Laboratory to verify that all species had the appropriate number of imaginary frequencies. For the identity proton-transfer reaction between benzene and its conjugate base, and for the nonidentity reactions between benzene and NH_2^-, benzene and CH_3NH^-, and between propyne and CH_3O^-, only the HF frequencies were obtained because of insufficient computational resources. Two of the ion−molecule complexes, those formed from propene plus allyl anion and from allene and allenyl (propargyl) anion, were computed to have one or more imaginary frequencies, $i\nu = -11$ cm^{-1} or lower

(22) (a) Keeffe, J. R.; Morey, J.; Palmer, C. A.; Lee, J. C. *J. Am. Chem. Soc.* **1979**, *101*, 1295. (b) Keeffe, J. R.; Yrigoyen, L. San Francisco State University, unpublished results. (c) Gandler, J. R.; Saunders, O. L.; Barbosa, R. *J. Org. Chem.* **1997**, *62*, 4677. (d) Gandler, J. R.; Bernasconi, C. F. *J. Am. Chem. Soc.* **1992**, *114*, 631. (e) Cox, B. G.; Gibson, A. *Chem. Commun.* **1974**, 683. (f) Cox, B. G.; Gibson, A. *Chem. Soc. Faraday Symp.* **1975**, *10*, 107.

(23) Pauling, L. *J. Am. Chem. Soc.* **1947**, *69*, 542. See also ref 23 of: Yoo, H. Y.; Houk, K. N. *J. Am. Chem. Soc.* **1994**, *116*, 12047.

(24) References 10d, 11b, 12a, 12f, and 12g. The same picture has been used to explain the relative slowness of carbon-centered nucleophiles and nucleofuges in nucleophilic substitution reactions at saturated carbon: Dedieu, A.; Veillard, A. *J. Am. Chem. Soc.* **1972**, *94*, 6730. Bader, R. F. W.; Duke, A.; Messer, R. R. *J. Am. Chem. Soc.* **1973**, *95*, 7715. Pellerite, M. J.; Brauman, J. I. *J. Am. Chem. Soc.* **1983**, *105*, 2672. Chabinyc, M. L.; Craig, S. L.; Regan, C. K.; Brauman, J. I. *Science* **1998**, *279*, 1882. Cao, W.; Erden, I.; Grow, R. H.; Keeffe, J. R.; Song, J.; Trudell, M. B.; Wadsworth, T. L.; Xu, F.-P.; Zheng, J.-B. *Can. J. Chem.* **1999**, *77*, 1009.

(25) Barone, V.; Cossi, M. *J. Phys. Chem. A* **1998**, *102*, 1995.

(26) Wavefunction, Inc., 18401 Von Karman Avenue, Suite 370, Irvine, CA 92612.

at the HF level, which are associated with torsional motions. One transition state, that for proton transfer from ethylsilane to ethylsilyl anion, had an extra imaginary frequency at $i\nu = -20$ cm^{-1}. The energetic effects are inconsequential relative to the total energies.

Additionally, the MP2/6-311+G** geometries were used to obtain single-point energies for most species at the following levels: B3LYP/6-311++G**, B3LYP/aug-cc-pvdz, coupled-cluster CCSD(T)/6-311+G**, and the CPCM polarizable continuum aqueous solvent model coupled to B3LYP/6-311++G**, hereafter called COSMO.[25] The electronic energies calculated by these methods are tabulated in Table S1 of the Supporting Information.[29] These results agree with published values where comparisons are possible. All energies were corrected for zero-point vibrational energies (ZPVE) as calculated at HF/6-311+G** and scaled by 0.9135.[30] No thermal corrections were made to the resulting enthalpies.

The multiparameter relationships between substituent constants and computed ΔH values were obtained by the use of "Solver" within the Excel spreadsheet software package.

Results

General. Some of the systems examined in this work have been investigated by computation previously. Proton transfer from the propargyl carbon of methylacetylene has been computed by Bernasconi and Wenzel.[11d] The allyl-to-allyl proton transfer has been studied by them[11d] and by Saunders and Shaik.[12f] The identity proton transfer to allenyl (propargyl) anion from allene was reported by Bernasconi and Wenzel.[11c] Nitromethane was studied by Bernasconi et al.,[11b] while the nitromethane to *aci*-nitromethane tautomerization energy was computed by Lammertsma and Prasad.[31] Proton transfer between acetaldehyde and its enolate was examined by Saunders[12b,f] and by Bernasconi and Wenzel.[11a] The acetonitrile reaction was similarly studied.[11b,12c] Proton transfer between methanol and methoxide was computed by Wolfe et al.,[10b] and by Van Verth and Saunders.[12e] Computational work on the ion−molecule complexes associated with proton-transfer reactions between heteroatoms is well known, especially for X = oxygen.[10a,b,12e,32] Chabinyc and Brauman have calculated the stationary points on the potential energy surfaces for the reaction between methoxide ion and both acetylene and phenylacetylene.[32] Much less has been reported on complexes between C−H acids and carbon-centered anions.[33]

Small differences between some of our ΔH values and those reported elsewhere using comparable methods[11] are attributable to our use of ZPVEs calculated at the HF level and to the fact that we have not made thermal corrections to 298 K.

Energetics. Calculated and experimental heats of deprotonation (ΔH_{ACID}) for the proton donors used in this study are listed in Table 1. These results allowed assessment of our computational methods as gauged by experiment. Linear correlations between experimental gas-phase ΔH_{ACID} values and those calculated by us are excellent, with r^2 better than 0.99 for all four gas-phase methods. The correlation between aqueous pK_a values and ΔH_{ACID} calculated using the COSMO solvent model is also good, better than that between the experimental gas-phase and COSMO values. The equations defining the correlations and the r^2 values are given in Table 2 where it will be seen that the MP2/6-311+G** method gives absolute values closest to the experimental results on average. In our subsequent discussion, MP2 ΔH values will be used unless otherwise indicated. Enthalpies of reaction for two isomerizations and three nonidentity proton transfers are found in Table 1 as well.

The heats of complexation (ΔH_{CX}) and activation ($\Delta H^{\ddagger}$) are defined as heats of formation of the anion−molecule complex and transition state, respectively, from the separated reactants. These complexation and activation energies are found in Table 3. None of the $\Delta H^{\ddagger}$ values and few of the ΔH_{CX} values have experimental counterparts. However, those for the complexation reactions between ethanol, methanol, acetonitrile and their respective conjugate bases are known and accord well with the computed figures; see Table 3. All of these results lend confidence to a discussion of our computed complexation energies and activation barriers, especially trends in these data.

Geometries. MP2/6-311+G** geometries calculated in this work are available as Cartesian coordinates upon request. Selected geometric features of reactants, complexes, and transition states can also be found in Table 4.

(1) Reactants. Several of the calculated structures are unusual enough to warrant special mention. Nitromethane anion, $CH_2{=}NO_2^-$, is calculated at MP2/6-311+G** to be slightly pyramidal at the carbon, a result observed previously.[11b,31] This structure has dihedral angles, H−C, N−O, of 7.7°, and is 16 cal/mol lower in electronic energy than the planar anion. The other methods all yielded a flat geometry for nitromethane anion. Similarly, allyl anion with the MP2/6-311+G**, COSMO, and CCSD(T) methods (but not with DFT) is slightly pyramidal at carbons 1 and 3 as was also found by Bernasconi and Wenzel.[11d] At the MP2 level, the pyramidal C2 structure is 33 cal/mol lower in electronic energy than the planar C_{2v} structure. Acetonitrile anion is also pyramidal at the deprotonated carbon. Moreover, it is not exactly linear, having a C−C−N angle of 176.4°. Bernasconi and Wenzel calculate the planar anion to be an inversion transition state lying less than 0.5 kcal/mol above the

(27) Frisch, M. J.; Trucks, G. W.; Schlegel, H. B.; Gill, P. M. W.; Johnson, B. G.; Robb, M. A.; Cheeseman, J. R.; Keith, T.; Petersson, G. A.; Montgomery, J. A.; Raghavachari, K.; Al-Laham, M. A.; Zakrzewski, V. G.; Ortiz, J. V.; Foresman, J. B.; Cioslowski, J.; Stefanov, B. B.; Nanayakkara, A.; Challacombe, M.; Peng, C. Y.; Ayala, P. Y.; Chen, W.; Wong, M. W.; Andres, J. L.; Replogle, E. S.; Gomperts, R.; Martin, R. L.; Fox, D. J.; Binkley, J. S.; Defrees, D. J.; Baker, M. J.; Stewart, J. P.; Head-Gordon, M.; Gonzalez, C.; Pople, J. A. *Gaussian 94*, revision E.2; Gaussian, Inc.: Pittsburgh, PA, 1995.

(28) Frisch, M. J.; Trucks, G. W.; Schlegel, H. B.; Scuseria, G. E.; Robb, M. A.; Cheeseman, J. R.; Zakrzewski, V. G.; Montgomery, J. A., Jr.; Stratmann, R. E.; Burant, J. C.; Dapprich, S.; Millam, J. M.; Daniels, A. D.; Kudin, K. N.; Strain, M. C.; Farkas, O.; Tomasi, J.; Barone, V.; Cossi, M.; Cammi, R.; Mennucci, B.; Pomelli, C.; Adamo, C.; Clifford, S.; Ochterski, J.; Petersson, G. A.; Ayala, P. Y.; Cui, Q.; Morokuma, K.; Salvador, P.; Dannenberg, J. J.; Malick, D. K.; Rabuck, A. D.; Raghavachari, K.; Foresman, J. B.; Cioslowski, J.; Ortiz, J. V.; Baboul, A. G.; Stefanov, B. B.; Liu, G.; Liashenko, A.; Piskorz, P.; Komaromi, I.; Gomperts, R.; Martin, R. L.; Fox, D. J.; Keith, T.; Al-Laham, M. A.; Peng, C. Y.; Nanayakkara, A.; Challacombe, M.; Gill, P. M. W.; Johnson, B.; Chen, W.; Wong, M. W.; Andres, J. L.; Gonzalez, C.; Head-Gordon, M.; Replogle, E. S.; Pople, J. A. *Gaussian 98*, revision A.11; Gaussian, Inc.: Pittsburgh, PA, 2001.

(29) See paragraph concerning Supporting Information at the end of this paper.

(30) Scott, A. P.; Radom, L. *J. Phys. Chem.* **1996**, *100*, 16502. The use of zero-point vibrational energies calculated at the MP2/6-311+G** level (rather than the HF level) and applied to MP2/6-311+G** electronic energies leads to an average difference in 50 computed ΔH_{ACID} and $\Delta H^{\ddagger}$ values of 0.1 ± 0.6 kcal/mol using data from this work and from refs 11c and 11d. For reactions involving the nonplanar allyl anion and the nonplanar nitromethide anion, we also used MP2 frequencies to obtain ΔH values. The same holds for the other nitroalkane reactions (except for the microhydration reactions) because differences between their calculated ΔH values are small and can be affected by the choice of ZPVE values.

(31) Lammertsma, K.; Prasad, B. V. *J. Am. Chem. Soc.* **1993**, *115*, 2348.

(32) Chabinyc, M. L.; Brauman, J. I. *J. Am. Chem. Soc.* **2000**, *122*, 5371.

(33) See, however, ref 9j; also see: (a) Cybulski, S. M.; Scheiner, S. *J. Am. Chem. Soc.* **1987**, *109*, 4199. (b) Chabinyc, M. L.; Brauman, J. I. *J. Am. Chem. Soc.* **2000**, *122*, 8739.

Table 1. Heats of Deprotonation, Isomerization, and Reaction (kcal/mol, 298 K): Experimental[a] and Computed[b,c]

system, R–**H**	ΔH_{RXN}(exp)	MP2/ 6-311+G**	B3LYP/ 6-311++G**	B3LYP/ cc-pvdz	COSMO AQ B3LYP/6-311++G**[h]	CCSD(T)/ 6-311+G**
		Deprotonation				
1. $CH_3C{\equiv}C\mathbf{H}$	381.1 ± 2.1	382.3	381.8	379.5	42.9	383.2
2. $HC{\equiv}CCH_2\mathbf{H}$	382.7 ± 3	385.4	378.7	376.3	57.9	386.3
3. $CH_3CH{=}CH\mathbf{H}$[d]	409.4 ± 0.6	408.1	407.1	405.2	80.2	409.2
	407.5 ± 2.0					
	409.0 ± 4.0					
4. $H_2C{=}CHCH_2\mathbf{H}$	389.1 ± 2.0	390.0 (389.5)	386.4	384.4	59.1	393.6
	390.7 ± 2.0					
5. $H_2C{=}C{=}CH\mathbf{H}$	381.1 ± 3	380.7	381.0	379.6	58.7	385.1
6. $CH_3CH_2CH_2\mathbf{H}$	419.4 ± 2.0	415.2	412.3	410.2	82.6	417.2
7. $C_6H_5\mathbf{H}$	401.7 ± 0.5	398.5				
8. $O_2NCH_2\mathbf{H}$	356.4 ± 2.9	360.1 (359.7)	352.4	351.7	29.0	361.8
9. $O_2NCH\mathbf{H}CH_3$	355.9 ± 2.2	359.8 (359.2)	351.4	350.8	27.8	361.1
10. $O_2NC\mathbf{H}(CH_3)_2$	356.0 ± 2.2	360.7 (360.7)	352.9	352.4	29.8	362.9
11. $O{=}NCH_2\mathbf{H}$	NA	352.3[e]				
12. $CF_3CH_2\mathbf{H}$[6]	NA	384.0	379.9	379.4	59.4	387.0
13. $O{=}CHCH_2\mathbf{H}$	365.8 ± 2.2	367.5	363.3	361.9	38.9	371.1
	366.5 ± 2.9					
14. $N{\equiv}CCH_2\mathbf{H}$	372.9 ± 2.1	374.5	369.6	368.3	46.1	377.1
	373.3 ± 2.6					
	374.8 ± 2.0					
15. $CH_3SO_2CH_2\mathbf{H}$	365.8 ± 2.2	367.5				
	366.5 ± 2.4					
16. $H_2C{=}NO_2\mathbf{H}$[f]	342.3 ± 2.9	341.5	338.2	338.0	14.2	344.7
17. $CH_3CH_2O\mathbf{H}$	378.3 ± 1.0	378.9	374.6	373.7	34.6	381.5
18. $CH_3O\mathbf{H}$	382.0 ± 1.0	381.8				
19. $CH_3CH_2NH\mathbf{H}$	399.3 ± 1.1	399.3	397.2	395.4	58.7	401.9
20. $CH_3NH\mathbf{H}$	403.2 ± 0.8	402.5				
$NH_2\mathbf{H}$	404.3 ± 0.3	403.6				
21. $CH_3CH_2SiH_2\mathbf{H}$[g]	385.4 ± 4.1	379.5	375.7	373.1		379.8
	378.0 ± 2.1					
		Isomerization				
$CH_3C{\equiv}CH \rightarrow H_2C{=}C{=}CH_2$	1.6 ± 3	4.8	−2.3	−3 4	−0.8	1.2
$CH_3NO_2 \rightarrow H_2C{=}NO_2H$[e]	14.1[f]	19.4	14.2	13.7	14.4	17.2
		Reaction				
$CH_3O^- + CH_3C{\equiv}C\mathbf{H} \rightarrow CH_3O\mathbf{H} + CH_3C{\equiv}C^-$	−0.9 ± 2.3	−0.3 (−0.2)[h]				
$NH_2^- + C_6H_5\mathbf{H} \rightarrow NH_2\mathbf{H} + C_6H_5$	−2.6 ± 0.6	−5.9				
$CH_3NH^- + C_6H_5\mathbf{H} \rightarrow CH_3NH\mathbf{H} + C_6H_5^-$	−1.5 ± 0.9	−4.8				

[a] Experimental values are taken from the NIST database except where indicated otherwise: Bartmess, J. E. In *NIST Standard Reference Database Number 69*; Mallard, W. G., Linstrom, P. J., Eds.; National Institute of Standards and Technology (http://webbook.nist.gov): Gaithersburg, MD, 1999. [b] All energies pertain to geometries optimized at MP2/6-311+G** except where otherwise indicated. [c] Corrections were made for zero-point vibrational energies calculated at HF/6-311+G** and scaled by 0.9135. ΔH values for reactions involving the nonplanar allyl anion, the nonplanar nitromethide anion, and the reactions of nitroethane and 2-nitropropane were also calculated using ZPVE values obtained at the MP2 level (see ref 30) and were scaled by 0.96: Pople, J. A.; Scott, A. P.; Long, J. W.; Radom, L. *Isr. J. Chem.* **1995**, *33*, 345. The resulting ΔH values are shown in parentheses. The COSMO values were calculated for the reaction $R{-}\mathbf{H} + H_2O \rightarrow R^- + H_3O^+$. [d] The first two entries under ΔH_{RXN} (exp) are for ethylene; the third is for *tert*-butylethylene. [e] Calculated from data provided by: Bernasconi, C. F.; Wenzel, P. J., personal communication. [f] No experimental value is available. The quoted value is a G2 ΔE result for nitromethane isomerizing to *aci*-nitromethane: Lammertsma, K.; Prasad, B. V. *J. Am. Chem. Soc.* **1994**, *116*, 642. [g] No experimental value is available. The values quoted for ethylsilane are for methylsilane.[a] [h] Computed at MP2/6-311+G**//HF6-311+G**.

stable state.[11d] The allenyl (propargyl) anion, the conjugate base common to allene and propyne (proton loss from methyl group), although planar about the CH_2 carbon, is bent about the central carbon and about the C−H carbon.[11c] The angles are 172.4° and 125.7°, respectively.

Relative to their conjugate acids, all but one of the anions, $A{-}B{-}X^-$, show an increase in bond length between atoms B and A. This is true for saturated as well as unsaturated anions. For the saturated anions (those in which A−B represents a formally single bond), the hyperconjugative extension of the A−B bond is most pronounced when atom A is conformationally anti to the lone pair. This feature is expressed most dramatically by the conjugate base of 1,1,1-trifluoroethane in which the C−F bond anti to the lone pair orbital has lengthened by 0.124 Å while the other two C−F bonds have become only 0.033 Å longer. The anion of dimethyl sulfone shows similar features. It is also pyramidal at the anionic carbon with significant extension of the $S{-}CH_3$ bond anti to the lone pair: that bond is 0.044 Å longer than in the neutral. Similarly, the S−O bonds are longer by 0.026 Å. The single exception to this generalization is the C−C bond in $CH_3CH_2SiH_2^-$ anion; it is essentially unchanged from that in the neutral.

Almost all of the anions also show a contraction of the X−B bond. The only exceptions are the ethylsilyl anion, the methylacetylide anion, the 1-propenyl anion, and the phenyl anion. The latter three have in common an anionic lone pair orthogonal to the adjacent π system.

(2) Transition States. The transition state for the allyl-to-allyl proton transfer calculated at the MP2/6-311+G** level (although not at HF/6-311+G**) is decidedly unsymmetrical. The distances between the two carbon termini and the proton in flight differ by 0.033 Å, and the two allyl moieties differ somewhat in geometry and charge distribution. The calculated ion−molecule complex preceding this transition state is chiral, and proton transfer within this complex leads to a product complex (not calculated) which is diastereomeric with the

Table 2. Correlations between Computed and Experimental Enthalpies of Deprotonation[a,b] for Identity Proton-Transfer Reactions

method	equation	*n*	r^2	average $\Delta H_{exp} - \Delta H$
MP2/6-311+G**	$\Delta H = 0.928\Delta H(\text{exp}) + 27.921$	21	0.994	-0.4 ± 2.2
B3LYP/6-311++G**	$\Delta H = 1.001\Delta H(\text{exp}) - 3.45$	15	0.992	3.1 ± 1.4
B3LYP/cc-pvdz	$\Delta H = 0.974\Delta H(\text{exp}) + 5.0815$	15	0.992	4.7 ± 1.6
CCSD(T)/6-311+G**	$\Delta H = 0.923\Delta H(\text{exp}) + 32.315$	15	0.994	-3.1 ± 2.2
CPCM-B3LYP/6-311++G**[c] (COSMO)	$\Delta H = 1.288pK_a(\text{aq}) + 14.515$	15	0.940[d]	NA

[a] All computations used optimized MP2/6-311+G** geometries. ΔE values were corrected for zero-point vibrational energy differences calculated at HF/6-311+G** and were scaled by 0.9135 except as noted in the text (ref 30): Pople, J. A.; Scott, A. P.; Long, M. W.; Radom, L. *Isr. J. Chem.* **1995**, *33*, 345. [b] Experimental gas-phase ΔH_{ACID} values were taken from: Bartmess, J. E. In *NIST Standard Reference Database Number 69*; Mallard W. G., Linstrom, P. J., Eds.; National Institute of Standards and Technology (http://webbook.nist.gov): Gaithersburg, MD, 1999. [c] The COSMO values were calculated for the reaction $R{-}H + H_2O \rightarrow R^- + H_3O^+$. [d] The correlation between the COSMO and experimental gas-phase ΔH values is not as good: $\Delta H_{COSMO} = 0.62\Delta H(\text{exp}) - 209$, $r^2 = 0.866$. Correlation between COSMO and MP2 values is slightly better: $\Delta H_{COSMO} = 0.95\Delta H(\text{MP2}) - 311$, $r^2 = 0.907$.

reactant complex. Thus, this reaction is not, strictly speaking, an identity reaction. Our unsymmetrical transition state lies only 0.15 kcal/mol lower than a symmetrical one calculated at the same level by Bernasconi and Wenzel.[11d] The transition states for the reactions between ethylamine and its anion, between benzene and its anion, and between nitroethane and its anion are very slightly unsymmetrical.

(3) Anion−Molecule Complexes. The geometries of the complexes calculated for the identity reactions in this study can be sorted into three groups, tight, moderate, and loose, determined by the identity (electronegativity) of the terminus atoms, X, between which the proton is to be transferred (see eqs 1 and 2), and by the complexation enthalpy, ΔH_{CX}. Tight complexes occur when X = oxygen. The complexes are strongly hydrogen-bonded with O−H distances ranging from 1.03 to 1.10 Å. These are longer than those in the uncomplexed neutral by 0.06 to 0.14 Å. The O···O nonbonded distances are only 2.43−2.52 Å, and the complexation energies are about 27.5 kcal/mol. All of these results indicate short, strong hydrogen bonding in the gas phase and are consistent with prior experimental and computational work on anion−molecule complexes between oxygen centers.[34] Moderate complexes are formed when X = N. The N−H distances are elongated by about 0.05 Å relative to the neutral, while the N···N distances are ca. 2.82 Å. Complexation energies are 16−17 kcal mol, and these complexes can also be characterized as hydrogen bonding. Looser complexes result when X = C. The C···C distances range from 3.27 Å (propyne + propynyl$^-$) to approximately 3.7 Å (propene + allyl$^-$). The greatest lengthening of a C−H bond occurring on complexation is that for the sp C−H bond of propyne which is extended by 0.037 Å in the complex. Other elongations are 0.014 Å or less except for the 0.02 Å increase which takes place when benzene complexes with phenyl anion. The larger C−H elongations are associated with the greater complexation energies, all about 8.5 kcal/mol for the hydrocarbon systems and greater than that for 1,1,1-trifluoroethane and acetonitrile. The remainder of the hydrocarbon C−H···C$^-$ complexes have ΔH_{CX} in the 4−5 kcal/mol range; see Table 3 for the complete list. The more stable complexes, according to their geometries, are weakly hydrogen-bonded C−H donor/C$^-$ acceptor complexes. Even the least stable ones show some H-bonding characteristics. For example, the neutral component in all of the hydrocarbon complexes has one unique hydrogen which, as compared to the isolated neutral, is notable either for its slightly greater C−H distance or for its increased positive charge, usually both. For highly resonance-stabilized carbanion acceptors such as allyl$^-$ and propargyl$^-$, the structures appear to have multiple long-range interactions.

The nitroalkanes, nitrosomethane, acetaldehyde, dimethyl sulfone, and ethylsilane are special cases. The most stable complexes formed between the nitromethide anion, the nitrosomethide anion, the acetaldehyde enolate anion, the dimethylsulfonyl anion and their respective conjugate acids are not C−H···C$^-$ complexes but C−H···O$^-$ complexes. These have complexation energies and C···O$^-$ distances which place them in the moderate or strong class. They do not lie directly on the proton-transfer pathway. We did not find a Si−H···Si$^-$ complex. Rather, the $Si^{\delta+}-H^{\delta-}$ hydrogen in the neutral avoids the negative silicon atom of the anion in favor of a C−H···Si$^-$ interaction, possibly the complex preceding the transfer of a proton from the CH_2 group of the neutral species to the silyl anion.

Three nonidentity reactions were studied. They were chosen to be very close to thermoneutral processes but with terminus atoms, X and X′, having different electronegativities. In each case, two complexes exist, a reactant complex and a product complex. For the reaction of propyne (acetylenic hydrogen) with methoxide, the C···O distances and the ΔH_{CX} values place the complexes at the higher end of the moderate category. Of the two complexes, the better donor/acceptor combination is OH···C$^-$ over CH···O$^-$. This result and our calculated complexation energy of 18.5 kcal/mol for $CH_3OH\cdots{}^-C{\equiv}CCH_3$ are in good agreement with results of Chabynic and Brauman.[32] The other two nonidentity reactions studied were those of benzene with two nitrogen bases, NH_2^- and CH_3NH^-. The four complexes are slightly looser and have smaller complexation energies than those formed in the propyne/methoxide system. In these cases, the CH···N$^-$ complexes are 3−5 kcal/mol more stable than the NH···C$^-$ complexes, both relative to their components.

Charges. Atomic charges computed by the natural population analysis (NPA) method were used to obtain atomic and group charges for portions of the reactants, complexes, and transition states. The resulting values are listed in Table S2 of the Supporting Information.[29] The charges on the acidic proton (q**H**) in both the transition state and the complex are also included in Table 4. The group charges were, in turn, used to calculate the components of the charge-based transition state imbalance (TSI) parameter, *n*, defined by Bernasconi.[11] The various components are given in Table S3 of the Supporting Information,[29] and the resulting *n* values are found in Table 5. We were unable to obtain NPA charges using the MP2/6-311+G** basis set for benzene, for the complex and transition state for methylacetylene plus methylacetylide anion, and for the transition states for benzene plus its anion, and for benzene plus dimethylamine anion. The necessary natural bond orbital analysis cannot handle linearly dependent basis sets.

(34) (a) McAllister, M. A. *Can. J. Chem.* **1997**, *75*, 1195. (b) Chen, J. G.; McAllister, M. A.; Lee, J. K.; Houk, K. N. *J. Org. Chem.* **1998**, *63*, 4611 and references therein.

Table 3. Calculated Heats of Complexation and Activation for Identity Proton-Transfer Reactions[a,b]

reactant acid	MP2/6-311+G**	B3LYP/6-311++G**	B3LYP/cc-pvdz	COSMO AQ B3LYP/6-311++G**	CCSD(T)/6-311+G**
1. $CH_3C{\equiv}C\mathbf{H}$					
complexation	−8.6	−8.4	−9.2	4.4	NA
activation	−4.1	−4.8	−7.2	18.1	NA
2. $HC{\equiv}CCH_2\mathbf{H}$					
complexation	−8.5	−6.7	−7.0	4.3	−8.2
activation	0.4	3.5	3.3	17.3	4.6
3. $CH_3CH{=}CH\mathbf{H}$					
complexation	−5.4	−3.7	−4.1	6.1	−5.2
activation	3.3	4.5	2.6	20.7	4.7
4. $H_2C{=}CHCH_2\mathbf{H}$					
complexation	−6.5	−3.4	−3.5	8.9	−6.2
activation	3.0 (3.8)	6.2	5.4	27.2	6.4
5. $H_2C{=}C{=}CH\mathbf{H}$					
complexation	−8.4	−6.5	−6.9	4.1	−7.9
activation	−3.5	−3.9	−5.2	10.9	−1.6
6. $CH_3CH_2CH_2\mathbf{H}$					
complexation	−3.9	−2.3	−2.8	7.0	NA
activation	4.5	5.4	4.3	28.2	5.5
7. $C_6H_5\mathbf{H}$					
complexation	−8.3				
activation	−2.2				
8. $O_2NCH_2\mathbf{H}$					
complexation[c]	−17.0	−16.9	−16.4	3.8	−17.9
activation	−8.4 (−7.9)	−9.0	−9.5	12.7	−5.5
anion + $2H_2O$	−30.1				
9. $O_2NCH\mathbf{H}CH_3$					
complexation[c]	NA				
activation	−9.8 (−9.0)			16.5	
anion + $2H_2O$	−30.7				
10. $O_2NC\mathbf{H}(CH_3)_2$					
complexation[c]	NA				
activation	−11.8			18.9	
anion + $2H_2O$	−31.4				
11. $O{=}NCH_2\mathbf{H}$[d]					
complexation[c]	∼ −14.6				
activation	−1.45				
12. $CF_3CH_2\mathbf{H}$					
complexation	−11.4	−10.0	−10.0	4.9	NA
activation	−4.5	−4.1	−4.6	14.6	NA
13. $O{=}CHCH_2\mathbf{H}$					
complexation[c]	−13.6	−11.4	−11.2	NA	−13.8
activation	−1.8	−2.7	−3.2	14.4	0.9
14. $N{\equiv}CCH_2\mathbf{H}$					
complexation	−14.2[e]	−12.7	−13.1	4.3	−13.9
activation	−9.0	−9.1	−9.8	11.1	−7.2
15. $CH_3SO_2CH_2\mathbf{H}$					
complexation[c]	−22.9				
activation	−10.7				
16. $H_2C{=}NO_2\mathbf{H}$					
complexation	−27.7	−25.2	−24.5	−4.1	−25.9
activation	−28.3	−25.1	−24.6	−3.4	−28.8
17. $CH_3CH_2O\mathbf{H}$					
complexation	−27.3[f]	−23.4	−23.5	6.0	−26.9
activation	−29.5	−26.1	−26.2	2.3	−28.9
18.$CH_3O\mathbf{H}$					
complexation	−27.15[f]				
activation	−30.07				
19. $CH_3CH_2NH\mathbf{H}$					
complexation	−16.6	−14.6	−14.2	6.1	−16.6
activation	−16.2	−14.2	−14.0	13.2	−15.4
20. $CH_3NH\mathbf{H}$					
complexation	−16.0				
activation	−15.8				
21. $CH_3CH_2SiH_2\mathbf{H}$					
complexation[c]	−5.2				
activation	11.6	10.3	10.6	NA	11.7
22. $CH_3O^- + CH_3C{\equiv}C\mathbf{H}$[g]					
complexation (r)	−14.6				
activation	−19.2, −19.0[h]				
complexation (p)	−18.5[h,i]				
23. $NH_2^- + C_6H_5\mathbf{H}$					
complexation (r)	−14.1				
activation	−11.3, −5.6[h]				
complexation (p)	−9.2[h]				

Table 3 (Continued)

reactant acid	MP2/6-311+G**	B3LYP/6-311++G**	B3LYP/cc-pvdz	COSMO AQ B3LYP/6-311++G**	CCSD(T)/6-311+G**
24. $CH_3NH^- + C_6H_5$**H**					
complexation (r)	−13.8				
activation	−12.7, −7.9[h]				
complexation (p)	−10.8[h]				

[a] All enthalpies of reaction and activation pertain to geometries optimized at MP2/6-311+G** except where otherwise noted. [b] Corrections were made for zero-point vibrational energies calculated at HF/6-311+G** and scaled by 0.9135. Heats of reaction and activation involving the nonplanar allyl anion, the nonplanar nitromethide anion, and the reactions of nitroethane were also calculated using ZPVE values obtained at the MP2 level (see ref 30), scaled by 0.96: Pople, J. A.; Scott, A. P.; Long, M. W.; Radom, L. *Isr. J. Chem.* **1995**, *33*, 345. The resulting ΔH values are shown in parentheses. [c] The complexes for the nitroalkanes, nitrosomethane, acetaldehyde, dimethyl sulfone, and ethylsilane are not X−H··· X^- complexes and do not lie on the reaction path for the identity proton-transfer reaction. [d] Calculated from data provided by Bernasconi, C. F.; Wenzel, P. J., personal communication, except for the complex (this work). [e] An experimental gas-phase complexation enthalpy, ΔH_{CX} (exp) = −12.8 kcal/mol, has been reported: Meot-Ner, M. *J. Amer. Chem. Soc.* **1988**, *110*, 3858. [f] Experimental complexation energies of −29.3 and −28.1 kcal/mol for methanol and ethanol, respectively, are reported by: Dodd, J. A.; Baer, S.; Moylan, C. R.; Brauman, J. I. *J. Am. Chem. Soc.* **1991**, *113*, 5942. [g] Computed at MP2/6-311+G**//HF6-311+G**. [h] These are the heats of formation of the product complexes or transition states from the products. [i] Heats of complexation between methanol and several alkynes are reported by: Chabynic, M. L.; Brauman, J. I. *J. Phys. Chem. A* **1999**, *103*, 9163; *J. Amer. Chem. Soc.* **2000**, *122*, 5371. These values average about −21 kcal/mol.

Discussion

Calculated Reaction Energy Surfaces. For proton-transfer reactions involving an oxygen center, including the nonidentity reaction between propyne and methoxide ion, the calculated transition state energies, corrected for zero-point vibrational energy, lie at or below that of the complex (the less stable complex in the case of the nonidentity reaction). It is not possible to distinguish between the transition state and this complex, and these reactions are best described as having "barrierless" single-well surfaces. The transfer of the proton is probably dominated by tunneling. For the propyne-to-methoxide proton transfer, the lowest energy structure is the hydrogen-bonded complex, $CH_3OH\cdots{}^-C{\equiv}CCH_3$, in which the O−H distance is just 0.05 Å longer than that in methanol. This result is almost identical to that found by Chabynic and Brauman for some closely related reactions.[33b]

For the nitrogen-to-nitrogen proton transfers, the transition states are 0.2 (methylamine) and 0.8 kcal/mol (ethylamine) higher than the complex. The carbon-to-nitrogen transfer from benzene to CH_3NH^- has a calculated transition state lying only 1.2 kcal/mol above the preceding complex. Because these results refer to conditions at 0 K, it is likely that at ordinary experimental temperatures sufficient thermal energy is available for the energy surfaces to behave effectively as single-well surfaces. However, the reaction between benzene and NH_2^- has its computed transition state 2.8 kcal/mol higher than the complex (for the reverse reaction, the figure is 3.6 kcal/mol); thus this reaction appears to have a double-well surface with a small but genuine barrier separating the complexes at experimentally accessible temperatures.

The other processes are identity reactions with X = carbon. In all cases, the transition states lie above the complex by 4.5 kcal/mol or more, characterizing these as double-well surfaces.

Correlations Involving ΔH Values. An attempted linear correlation between calculated (MP2) ΔH_{ACID} and $\Delta H^{\ddagger}$ values showed essentially no correlation when all 21 identity reactions were used. By culling subsets from the data, better linear relationships could be found. For example, a subset composed of methanol, ethanol, methylamine, ethylamine, and propane, that is, a set without polar Y groups (see eq 1), shows a fairly good correlation: $\Delta H^{\ddagger} = 0.90\Delta H_{ACID} - 373$, with $r^2 = 0.934$. Another subset composed of all of the C−H acids gives a very poor correlation. However, a smaller group including methylacetylene (acetylenic hydrogen), propene (olefinic hydrogen), allene, nitromethane, 1,1,1-trifluoroethane, and propane (methyl hydrogen) coincidentally shows a good correlation, see Figure 1, with $\Delta H^{\ddagger} = 0.25\Delta H_{ACID} - 97$, $r^2 = 0.976$. The slope and intercept of this plot are much different than those found for the nonpolar subset reflecting the lack of mutual fit. From Figure 1, one also sees that the identity proton-transfer reactions of acetonitrile, benzene, nitroethane, 2-nitropropane, and dimethyl sulfone have lower barriers than those predicted from the correlation. On the other hand, the reactions of acetaldehyde, propyne (propargylic hydrogen), propene (allylic hydrogen), and especially nitrosomethane have higher barriers, the last by 9.4 kcal/mol.

Good linear correlations between equilibrium and kinetic acidities are common for reactions in aqueous solution, sometimes extending over 25 log K_{eq} units (ca. 35 kcal/mol at 300 K).[35] These include the well-known Brönsted relationships found for rate controlling proton-transfer processes. In the gas phase, the separated reactants have no interactions with one another. At the transition state, the reactants experience interactions having no counterpart in the prior reactant state. Because the strength and nature of these interactions must vary from system to system, it would be surprising if a general correlation between gas-phase equilibrium and kinetic acidities were to exist. In solution, the separated reactants are surrounded by polar and polarizable matter, the solvent. The transition states are also surrounded by this matter; thus the reactant−reactant interactions, specific to each system, can be largely or completely dominated by solvation. This effect could attenuate differences in total interaction energy between reactant and transition states and contribute to a smoother correlation between acid strength and rates of proton transfer in solution.

The importance of intermoiety interactions in the gas phase is underlined by the excellent linear correlations we find between computed (MP2) complexation and activation enthalpies, see Figure 2. A set of 14 identity reactions including C−H, O−H, and N−H acids shows $\Delta H^{\ddagger} = 1.48\Delta H_{cx} + 10.6$ with $r^2 = 0.980$.[36] The other gas-phase methods also give good correlations between $\Delta H^{\ddagger}$ and ΔH_{cx} with r^2 values all above 0.95 for identity reactions. Inclusion of MP2 results for the six nonidentity reactions from our study barely affects the MP2 correlation: $\Delta H^{\ddagger} = 1.49\Delta H_{cx} + 9.8$, $r^2 = 0.946$.[37] It is evident that

(35) Keeffe, J. R.; Kresge, A. J. In *The Chemistry of Enamines*; Rappoport, Z., Ed.; Wiley-Interscience: New York, 1994; Chapter 19. See also the useful data in: MacCormack, A. C.; McDonnell, C. M.; More OFerrall, R. A.; O'Donoghue, A. C.; Rao, S. N. *J. Am. Chem. Soc.* **2002**, *124*, 8575.

Table 4. Selected Bond Lengths of Molecules in This Study (Å) and NPA Acidic Proton Charges for Complexes and Transition States in the Identity Proton Transfers (MP2/6-311+G**)

system, A–B–X–**H**	*d* (X–**H**)[a]	*d* (B–X)[b]	% change at TS, *d* (B–X)[c]	*q***H**
1. $CH_3C{\equiv}C\mathbf{H}$				
neutral	1.064	1.218		
complex	1.101	1.224		NA[d]
ts	1.404	1.246	65	NA[d]
anion	NA	1.261		
2. $HC{\equiv}CCH_2\mathbf{H}$				
neutral	1.093	1.464		
complex	1.100	1.463		0.287
ts	1.420, 1.430	1.430	35	0.296
anion	NA	1.366		
3. $CH_3CH{=}CH\mathbf{H}$				
neutral	1.085	1.341		
complex	1.098	1.342		0.261
ts	1.423	1.351	53	0.259
anion	NA	1.360		
4. $H_2C{=}CHCH_2\mathbf{H}$				
neutral	1.094	1.502		
complex	1.097	1.504		0.238
ts[d]	1.394, 1.427	1.447, 1.444	53, 56	0.254
anion	NA	1.399		
5. $H_2C{=}C{=}CH\mathbf{H}$				
neutral	1.086	1.314		
complex	1.099	1.311		0.273
ts	1.399	1.295	58	0.266
anion	NA	1.281		
6. $CH_3CH_2CH_2\mathbf{H}$				
neutral	1.095	1.529		
complex	1.097	1.527		0.254
ts	1.439	1.516	68	0.277
anion	NA	1.510		
7. $C_6H_5\mathbf{H}$				
neutral	1.087	1.400		
complex	1.105	1.402		0.288
ts[d]	1.425, 1.434	1.411, 1.411	46	NA[d]
anion	NA	1.424		
8. $O_2NCH_2\mathbf{H}$				
neutral	1.088	1.493		
complex[e]	1.096	1.489		NA
ts	1.391	1.414	57	0.253
anion	NA	1.355		
9. $O_2NCH\mathbf{H}CH_3$				
neutral	1.091	1.499		
complex[e]				NA
ts[d]	1.379, 1.383	1.411, 1.410	61, 60	0.260
anion	NA	1.351		
10. $O_2NC\mathbf{H}(CH_3)_2$				
neutral	1.091	1.507		
complex[e]				NA
ts[d]	1.375	1.414	60	0.272
anion	NA	1.352		
11. $O{=}NCH_2\mathbf{H}$[f]				
neutral		1.480		
complex	1.141	1.442		NA
ts	1.402	1.368	70	0.260
anion	NA	1.320		
12. $CF_3CH_2\mathbf{H}$				
neutral	1.090	1.499		
complex	1.103	1.488		0.292
ts	1.433	1.456	52	0.294
anion	NA	1.417		
13. $O{=}CHCH_2\mathbf{H}$				
neutral	1.093	1.505		
complex[e]	1.097	1.500		NA
ts	1.418	1.430	65	0.300
anion	NA	1.390		
14. $N{\equiv}CCH_2\mathbf{H}$				
neutral	1.091	1.463		
complex	1.102	1.461		0.294
ts	1.420	1.431	54	0.303
anion	NA	1.404		
15. $CH_3SO_2CH_2\mathbf{H}$				
neutral	1.091	1.784		
complex[e]	1.090	1.774		NA
ts	1.427	1.730	45	0.294
anion	NA	1.665		
16. $H_2C{=}NO_2\mathbf{H}$[g]				
neutral	0.971	1.417		
complex	1.034	1.374		0.484
ts	1.202	1.343	52	0.452
anion	NA	1.278		
17. $CH_3CH_2O\mathbf{H}$				
neutral	0.961	1.426		
complex	1.072	1.395		0.480
ts	1.201	1.380	53	0.474
anion	NA	1.340		
18. $CH_3O\mathbf{H}$				
neutral	0.960	1.421		
complex	1.100	1.389		0.475
ts	1.201	1.381	53	0.470
anion	NA	1.345		
19. $CH_3CH_2NH\mathbf{H}$				
neutral	1.015	1.467		
complex	1.061	1.457		0.432
ts[d]	1.298, 1.299	1.443, 1.446	77, 68	0.407
anion	NA	1.436		
20. $CH_3NH\mathbf{H}$				
neutral	1.014	1.465		
complex	1.066	1.459		0.427
ts	1.302	1.452	62	0.399
anion	NA	1.444		
21. $CH_3CH_2SiH_2\mathbf{H}$				
neutral	1.480	1.882		
complex[e]				NA
ts	1.788	1.920	48	−0.147
anion	NA	1.961		

[a] The bond between the acidic proton and atom X. In the case of the ion−molecule complex, the distance is that within the neutral component. [b] The distance between reaction center X and the more electronegative attached heavy atom. In the complex, the distance is that within the neutral component. [c] Defined as the percent change in B−X length which has occurred from the neutral reactant to the transition state relative to the (greater) change occurring from the neutral reactant to the product anion. [d] Except for propyne + propynyl$^-$, these transition states are not quite symmetrical. See text under Results, Geometries, Transition States. We could not obtain charges for the benzene/benzene anion ts, nor for the propyne/propynyl anion complex or ts. [e] The complexes in these cases are not C−H···C$^-$ complexes, rather they are C−H···O$^-$ complexes, not on the carbon-to-carbon reaction coordinate. See text under Results, Geometries, Anion−Molecule Complexes. Similarly, the silane complex is not a Si···H···Si$^-$ complex but a C−H···Si$^-$ complex. Charges for these complexes are therefore not applicable. [f] Data taken from: Bernasconi, C. F.; Wenzel, P. J. *J. Org. Chem.* **2001**, *66*, 968−979, except for the complex (this work). [g] Neutral *aci*-nitromethane prefers the syn conformation about the O−N−O−H dihedral. The best complex is anti on one side and syn on the other, while the best transition state is anti−anti.

electrostatic/hydrogen-bonding forces, which stabilize the complexes, are manifest in the transition states as well.

Correlations Involving Charges. Qualitative support for the above claim is supplied by the excellent correlation between the MP2/6-311+G** NPA charges on the acidic proton in the complex, *q***H**(cx), and in the transition state, *q***H**‡, see Figure 3 and Table 4. This point is further supported by a monotonic correlation between $\Delta H^‡$ and *q***H**(cx), see Figure 4. It follows (see inset in Figure 4) that $\Delta H^‡$ and *q***H**‡ are also correlated.[38] The inset figure shows four "islands" of points, one each for

Table 5. Transition State Imbalance Parameters[a] for Identity Proton-Transfer Reactions Calculated from NPA Group Charges: $Y-X^- + H-X-Y \rightarrow [Y-X\cdots H\cdots X-Y]^{\ddagger} \rightarrow Y-X-H + {}^-X-Y$

system, Y–X–**H**[b]	MP2/6-311+G**	B3LYP/6-311++G** (cc-pvdz)	B3LYP/6-311++G**	CCSD(T)/6-311+G**	CPCM aq solvent model B3LYP/6-311++G**
1. $CH_3C{\equiv}C\mathbf{H}$	(1.11)[c]	1.10			
2. $HC{\equiv}CCH_2\mathbf{H}$	2.26	2.10	2.08	2.75	2.46
3. $CH_3CH{=}CH\mathbf{H}$	1.10	1.12	1.09	1.10	1.06
4. $H_2C{=}CHCH_2\mathbf{H}$[d]	1.62, 1.51	1.57, 1.50	1.55, 1.49	2.02, 2.02	1.62, 1.53
5. $H_2C{=}C{=}CH\mathbf{H}$	1.29	1.20			
6. $CH_3CH_2CH_2\mathbf{H}$	1.23	1.39	1.32	1.28	0.52
7. $C_6H_5\mathbf{H}$	NA				
8. $O_2NCH_2\mathbf{H}$[e]	1.58 (1.60)	(1.43)			
9. $O_2NC\mathbf{H}CH_3$	1.63				
10. $O_2NC\mathbf{H}(CH_3)_2$	1.68				
11. $O{=}NCH_2\mathbf{H}$[f]	1.28				
12. $CF_3CH_2\mathbf{H}$	1.70	1.45	1.49		1.67
13. $O{=}CHCH_2\mathbf{H}$	1.53	1.40	1.39	1.90	1.55
14. $N{\equiv}CCH_2\mathbf{H}$	1.50	1.44	1.43	1.82	1.55
15. $CH_3SO_2CH_2\mathbf{H}$	1.63				
16. $CH_2{=}NO_2\mathbf{H}$[e]	2.78 (2.76)	(2.89)			
17. $CH_3CH_2O\mathbf{H}$	2.50	2.89	2.72	2.57	1.80
18. $CH_3O\mathbf{H}$	2.39				
19. $CH_3CH_2NH\mathbf{H}$[d]	1.72, 1.58	2.00, 1.87	1.94, 1.82	1.98, 1.85	1.35, 1.35
20. $CH_3NH\mathbf{H}$	1.92				
21. $CH_3CH_2SiH_2\mathbf{H}$	0.57				
23. $NH_2^- + C_6H_5\mathbf{H}$[g]	1.04				
24. $CH_3NH^- + C_6H_5\mathbf{H}$[g]	1.07				
24a. $C_6H_5^- + CH_3NH_2\mathbf{H}$[g]	1.89				

[a] Definitions: $n = \log(\delta Y/\aleph)/\log(\delta_Y + \delta_X)$ is the transition state imbalance parameter introduced by Bernasconi, see: Bernasconi, C. F. *Acc. Chem. Res.* **1992**, *25*, 9. Further definitions: δ_Y = (charge on Y group(s) in transition state − charge on Y group(s) in Y−X−H); δ_X = (charge on $X(H)_{n-1}$ group in transition state − charge on $X(H)_n$ group in Y−X−H); $\aleph$ = (charge on Y group(s) in conjugate base − charge on Y group(s) in Y−X−H). Except for the transferred proton, all hydrogen charges are summed onto the attached heavy atom. See: Bernasconi, C. F.; Wenzel, P. J. *J. Am. Chem. Soc.* **1994**, *116*, 5405; *J. Org. Chem.* **2001**, *66*, 968 and references therein. All calculations use molecular geometries optimized at the MP2/6-311+G** level except where otherwise indicated. [b] Symbols: **H** is the proton transferred from atom X of the conjugate acid to atom X of the conjugate base. Y is the group(s), other than hydrogens, attached to atom X. [c] We were unable to obtain NPA charges for the propyne transition state at the MP2/6-311+G** level. The values quoted here in parentheses are interpolated from good to excellent correlations between MP2 and B3LYP-cc-pvdz values obtained for six or more systems in common. [d] The transition state for the allyl-to-allyl proton transfer calculated by us with the MP2/6-311+G** basis set is unsymmetrical, although that calculated at HF/6-311+G** is symmetrical. Bernasconi, C. F.; Wenzel, P. J. *J. Org. Chem.* **2001**, *66*, 968 report a symmetrical transition state at MP2/6-311+G** with an electronic energy 0.15 kcal/mol above our unsymmetrical one. The transition state imbalance parameter calculated from their data is $n = 1.61$. The transition states for identity proton-transfer reactions between ethylamine and its anion, benzene and its anion, and nitroethane and its anion are also slightly unsymmetrical. [e] The *n* values in parentheses for nitromethane and *aci*-nitromethane use charges calculated for the fully planar nitromethide anion. [f] The nitrosomethane results are calculated from data taken from Bernasconi and Wenzel, *J. Org. Chem.* **2001**, *66*, 968. That work also summarizes their computations on systems 2, 4, 5, 8, 13, and 14. [g] These are not identity reactions, but are close to thermoneutral (see Table 1). The significance of the TSIPs is not clear in these cases.

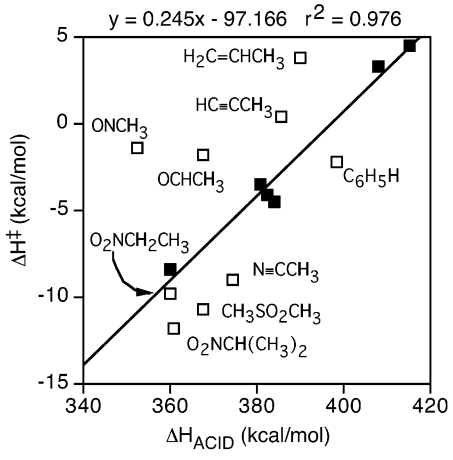

Figure 1. Plot of ΔH_{ACID} values versus $\Delta H^{\ddagger}$ values (MP2/6-311+G**) for C−H acids in this study. The line is defined by the points for propyne (acetylenic hydrogen), propene (vinylic hydrogen), allene, nitromethane, 1,1,1-trifluoroethane, and propane (methyl hydrogen).

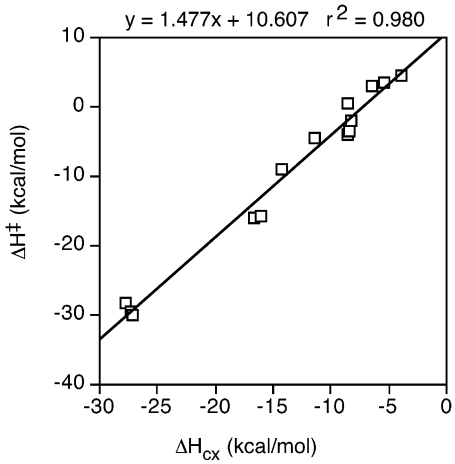

Figure 2. Plot of ΔH_{CX} values versus $\Delta H^{\ddagger}$ values (MP2/6-311+G**) for identity proton transfers of the C−H, N−H, and C−H acids in this study which have ion−molecule complexes leading to proton transfer.

O−H, N−H, C−H, and Si−H acids. The relationship is not unexpected given the prior demonstration that for the simple nonmetal hydrides of the first and second row elements transition state energy is well correlated with the integrated Bader population of the transferred hydrogen.[10d] We also note here that the charges on the proton in the ts calculated by the COSMO aqueous solvent model are extremely well correlated with the corresponding MP2 charges, $q\mathbf{H}^{\ddagger}(\text{COSMO}) = 1.15q\mathbf{H}^{\ddagger}(\text{MP2}) - 0.07$ ($r^2 = 0.998$), and that a plot of $q\mathbf{H}^{\ddagger}$(COSMO) against $\Delta H^{\ddagger}$(COSMO) strongly resembles that in Figure 4 (inset).

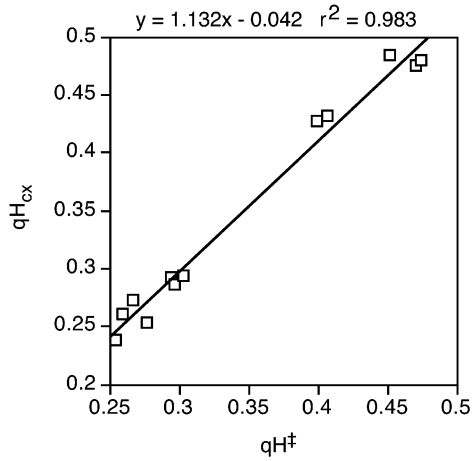

Figure 3. Plot of the charge on the transferred proton in the transition state ($q\mathbf{H}^{\ddagger}$) versus the charge on that proton in the ion−molecule complex ($q\mathbf{H}_{CX}$) leading to proton transfer for identity reactions of C−H, N−H, and O−H acids (MP2/6-311+G**).

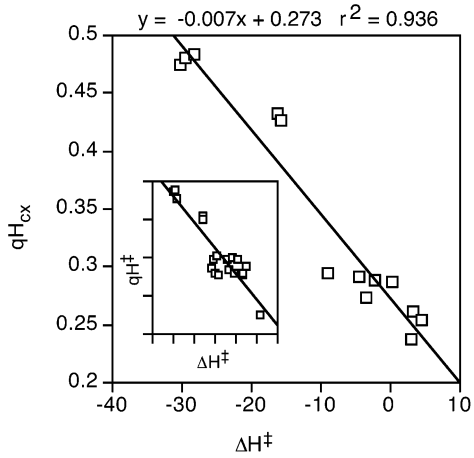

Figure 4. Plot of $\Delta H^{\ddagger}$ versus the charge on the proton to be transferred in the ion−molecule complex ($q\mathbf{H}_{CX}$) at MP2/6-311+G**. The inset shows a similar plot of $\Delta H^{\ddagger}$ versus $q\mathbf{H}^{\ddagger}$, the charge on the transferred proton in the transition state.

A general characteristic of the transition states for proton-transfer reactions may be inferred from the results presented to this point. These structures are stabilized by contributions from triple-ion electrostatic interactions (structure **2b**), the more so as X is more electronegative.[24] The example of ethylsilane is

$$[\underset{\mathbf{2a}}{Y{-}X{-}H\cdots{}^{-}X{-}Y} \Leftrightarrow \underset{\mathbf{2b}}{Y{-}X^{-}\ H^{+}\ {}^{-}X{-}Y} \Leftrightarrow \underset{\mathbf{2c}}{Y{-}X^{-}\cdots H{-}X{-}Y}]^{\ddagger}$$

instructive. Its activation barrier is the highest of the identity reactions studied by us. Moreover, the charge (absolute value) on the proton-in-flight in its transition state is the lowest ($q\mathbf{H}^{\ddagger}$ is, in fact, slightly negative). It is a general result that electronegativity is lower and identity proton-transfer activation barriers are higher for transfers between atoms in the second row of the periodic table than for those immediately above them in the first row. Gronert has explained this result noting that the Si−H bond is polarized in the sense $Y{-}Si^{\delta+}{-}H^{\delta-}$. Not only are its complexes with anionic bases weakened by this fact, but the Si−H bond must undergo partial reversal of its polarity for the hydrogen to be transferred as a proton. These changes come with an energetic cost.[10d]

Transition State Imbalance. As discussed in the Introduction, the issue of transition state imbalance (TSI), the failure of all bonding and solvation changes to develop in a synchronous fashion at the transition state, might be addressed computationally by examining both geometries and charges.

Fractional changes in bond lengths, angles, out-of-plane distances, and the like can be assessed by comparing the change that has occurred at the transition state with that reached at the product state, both referred to the reactant state. These measures of TSI are not likely to yield a unique figure because the various changes in geometry involve different types of motion with different force constants. Thus, a given geometric change might not have the same energetic consequences as another type of change. We report in Table 4 only the % change in the length of the bond between the atom undergoing deprotonation, X, and the more electronegative of the heavy atoms directly attached to X. For example, in the case of nitroethane, this change refers to the bond between carbon-1 and the nitrogen of the nitro group. We choose a % change in bond length because such changes are associated with larger force constants than are changes in angles, and hence affect bond strengths more strongly.

Fractional changes in atomic and group charges have been used by Bernasconi to devise a "transition state imbalance parameter" (TSIP) called *n*.[11] This parameter is defined, using the reaction formalism of eq 1, by eq 3; see also the footnotes to Table 5.

$$n = \log(\delta_Y/\aleph)/\log(\delta_Y + \delta_X) \qquad (3)$$

The components of eq 3 are changes in atomic and group charges, and thus: δ_Y = (charge on Y group(s) in transition state − charge on Y group(s) in neutral Y−X−H), δ_X = (charge on $X(H)_{n-1}$ group in transition state − charge on $X(H)_n$ group in $Y{-}X{-}H_n$), and $\aleph$ = (charge on Y group(s) in anion product − (charge on Y group(s) in neutral X−Y−H).

Except for the transferred proton, all hydrogen charges are summed onto the attached heavy atom. The definition of *n* is rational. For example, if delocalization of negative charge into the Y group of the anion were complete, and if one-half of this charge were in each Y group at the transition state, the numerator and denominator of eq 3 would be equal at log 0.5 and *n* would be 1.00, indicating no transition state imbalance. Imbalance leads to values greater than 1.0.

The resulting TSIPs are tabulated in Table 5. The first thing that stands out is that, even for systems in which π-electron delocalization in the anion and transition state is expected to be minimal or nonexistent, the TSIPs are element-dependent. For example, comparison of propyne, propene, and propane (entries 1, 3, and 6) with ethanol and methanol (entries 17 and

(36) The nitroalkanes, nitrosomethane, acetaldehyde, and dimethyl sulfone are excluded from the correlation. As discussed above, their ion−molecule complexes are different in structure from the others and are characterized by an attractive interaction between the negative oxygen(s) of the anion with the α-CH bond(s) of the neutral form. These complexes are significantly more stable than that expected for a C−H···C$^-$ structure. Similarly, the ethylsilane/silyl$^-$ complex is a C−H···Si$^-$ complex rather than a Si−H···Si$^-$ complex.

(37) Only the point for the reaction between propyne (acetylenic hydrogen) and methoxide ion seems somewhat aberrant; its removal raises r^2 to 0.970, almost the same as for the identity reactions alone.

(38) In fact, there is a fairly good correleation between the (average) charge on the acidic hydrogen in the neutral reactants and $\Delta H^{\ddagger}$, $r^2 = 0.90$.

18) and with ethylamine and methylamine (entries 19 and 20) shows that the more electronegative is reaction terminus X, the greater is the apparent imbalance. This result has an intuitively satisfying explanation, however. The greater the electronegativity of X, the greater will be the negative charge on X in the transition state and the less the delocalization into the attached Y group. It is not that there is extensive delocalization of charge in the anions of alcohols and amines, but that amount of delocalization must be substantially greater than in the transition state because in the ts the triple-ion contribution (see structure **2b** above) can enhance stability to a greater extent the more electronegative is X. In other words, this result is consistent with an important contribution from the triple-ion structure to the transition state, a conclusion further underlined by the greater positive charge on the proton-in-flight for these cases (see Table 4). This picture provides a useful explanation of the kinetic acidity order of the simple O−H, N−H, and C−H acids, particularly in the gas phase, and possibly in solution as well.

Further discussion of relative TSIP values therefore requires that comparisons be made between systems in which the reaction termini, X, are the same. For those C−H acids expected to have the least π-electron delocalization (relocation) in their conjugate bases, one does find values close to those expected for little or no imbalance at the transition state. A small amount of imbalance is indicated, however, by the results for allene, propane, and even for propyne (acetylenic H) and propene (vinylic H), consistent with σ-electron delocalization in the anion, less in the ts. The relatively large TSI associated with 1,1,1-trifluoroethane reflects the strong hyperconjugative interaction between the residual lone pair and the anti C−F bond in the anion (less strong in the ts), also indicated by the considerable elongation of that bond relative to the conjugate acid. Greater TSI is evident from the results for acids with π-delocalized anions, the largest amount, occurring for propyne ionizing at the methyl carbon to propargyl anion. This case has been discussed by Bernasconi and Wenzel.[11d] Thus, the relative TSIP values are "sensible" based on prior expectations. The same can be said of the O−H acids, although the only comparison possible here is between methanol and ethanol, on one hand, and *aci*-nitromethane on the other. The latter undergoes some π delocalization upon ionization and has TSIP values indicating a somewhat greater imbalance than for the simple alcohols.

There remain a few unexpected results to consider. Ethylsilane produces an *n* value that is outside the apparent limiting values for these parameters. This result might be a consequence of the fact that the ts for this reaction has hydride character at the hydrogen-in-flight. A second surprise is that the TSIPs calculated with the COSMO aqueous solvent model are not very different from the gas-phase parameters, particularly for the C−H acids. On the basis of previous experimental work in solution, particularly for the nitroalkanes (see the Introduction), we expected more TSI in solution, especially in hydrogen-bonding donor solvents. For ethanol and ethylamine, the computed TSIPs are actually smaller in solution than in the gas phase. Additionally, the *n* value computed for propane with COSMO lies outside the expected boundary value. It is not clear whether the solvent model is inadequate to the purpose or if a larger conceptual problem is the cause. However, it must be noted that COSMO does not supply specific molecular solvation, but rather a continuous dielectric environment.

Table 6. Acidities of the Simple Nitroalkanes in Various Media

compound	pK_a $(H_2O)^{a,b}$	pK_a $(DMSO)^{b,c}$	ΔH_{ACID} $(gas)^{d}$	ΔG_{ACID} $(gas)^{b,d}$
CH_3NO_2	10.70	17.68	356.4	350.3
$CH_3CH_2NO_2$	8.90	17.02	355.9	349.9
$(CH_3)_2CHNO_2$	7.74	16.88	356.0	350.0

[a] Nitromethane and nitroethane: Pearson, R. G.; Dillon, R. L. *J. Am. Chem. Soc.* **1953**, *75*, 2439. 2-Nitropropane: Turnbull, D.; Maron, S. H. *J. Am. Chem. Soc.* **1943**, *65*, 212. [b] pK_a and ΔG_{ACID} values are corrected for the number of hydrogens at the acidic site. [c] Bordwell, F. G.; Bartmess J. E.; Hautala, J. A. *J. Org. Chem.* **1978**, *43*, 3095. [d] In kcal/mol; Bartmess, J. E. In *NIST Standard Reference Database Number 69*; Mallard W. G., Linstrom, P. J., Eds.; National Institute of Standards and Technology (http://webbook.nist.gov): Gaithersburg, MD, 1999.

We make the following conclusions: (1) Charge-based, computed transition state imbalance values can be useful, but only when comparisons are made within reaction sets in which the reaction termini, X, are identical. (2) The gas-phase results are largely those expected a priori, although small but interesting surprises are provided by allene and 1,1,1-trifluoroethane. Such "surprises" may turn out to be the most valuable use of TSIPs. (3) Transition state imbalance in proton-transfer reactions exists because it allows a greater stabilizing effect from electrostatic/H-bonding interactions. Delocalization of charge away from the reaction termini, X, would compromise the strength of this interaction.

How do the charge-based TSIP values accord with geometry-based indicators of progress at the transition state? Not very well. The fractional contractions of the X−B bonds achieved at the transition state for the 14 C−H acids in this study tend to cluster between 50% and 60%, indicating fairly well-balanced transition states; see Table 4. Plots of the available *n* values against the % change in this bond length show poor correlations and much scatter. However, as Bernasconi has pointed out, there is no requirement that these measures of progress must track each other.[11a]

The Nitroalkane Anomaly. As discussed in the Introduction, there are two classic experimental examples of transition state imbalance, both having to do with deprotonation of nitroalkanes.[16−18] The magnitude of the anomaly is less in solvents unable to act as H-bonding donors to the negative oxygens of the nitronate anions.[22] In fact, the order of the acidities of nitromethane, nitroethane, and 2-nitropropane is itself solvent dependent, tending toward, if not reaching, the gas-phase order when the non-H-bonding donor solvent, DMSO, is used in place of water; see Table 6. Therefore, although experiment and computation indicate that TSI is ubiquitous, even in the gas phase, one may ask whether a "nitroalkane anomaly" exists in the gas phase.

This topic has recently been addressed by Yamataka et al.[9j] In water, nitroethane is 15 times more acidic than nitromethane, and yet it reacts with OH^-/H_2O 5 times more slowly. These workers measured rates and equilibria for the reactions of CH_3O^- with nitromethane and nitroethane in the gas phase. Under their conditions, nitroethane proved to be 0.2 kcal/mol more acidic and reacted at the same rate as nitromethane. Unfortunately, the observed rates were so close to the encounter limit that it is not clear whether a difference could have been measured. However, Yamataka et al. also made fairly high level calculations (B3LYP/6-31+G*) of the activation and reaction

free energies for the reaction of CN^- with three arylnitromethanes, the unsubstituted compound, and the *p*-methoxy and *p*-nitro derivatives. The resulting plot of $\Delta G^{\ddagger}$ versus ΔG_{RXN} was accurately linear with a slope, $\alpha = 0.51$, in marked contrast to the anomalous aqueous solution value of 1.3−1.5 (depending on the base used).[17,18]

We have looked at the issue in two ways. First, we carried out semiempirical AM1 calculations on the reaction of formate anion with 12 *meta* and *para* ring-substituted arylnitromethanes, eq 4.[39] A range of ΔH_{RXN} values of 25 kcal/mol was covered by this set, and a good rate-equilibrium correlation was found: $\Delta H^{\ddagger} = 0.55\Delta H_{RXN} + 2.4$; $r^2 = 0.979$. Although the computational level is not high, we are encouraged to accept this observation by its agreement with the higher level result obtained by Yamataka and co-workers. We also performed a more rigorous computational study at the MP2/6-311+G** level followed by single-point calculations using the COSMO solvation model in which equilibrium and kinetic acidities of nitromethane, nitroethane, and 2-nitropropane are compared. The computed ΔH_{ACID} and $\Delta H^{\ddagger}$ values are reported in Tables 1 and 3, respectively. The COSMO ΔH_{ACID} order is the same as the gas-phase order, but opposite to the experimental aqueous phase order. However, the COSMO $\Delta H^{\ddagger}$ order is nitromethane < nitroethane < 2-nitropropane, in agreement with aqueous results, but opposite to the computed gas-phase order. Thus, COSMO partially models the nitroalkane anomaly.

$$Ar{-}CH_2{-}NO_2 + HCO_2^- \rightarrow HCO_2H + Ar{-}CH{-}NO_2^- \quad \alpha(AM1) = 0.55 \quad (4)$$

Substituent Effects on ΔH_{ACID}, ΔH_{CX}, and $\Delta H^{\ddagger}$. In an earlier paper,[11b] we showed that computed gas-phase acidities and identity reaction activation barriers for a set of five C−H acids, $Y{-}CH_3$, could be well correlated with a dual substituent parameter treatment using the gas-phase substituent constants of Hansch, Leo, and Taft.[40] The parameters used were the field or polar effect (σ_F) and resonance effect (σ_R) substituent constants. The results showed that resonance effects dominated in determining the acidities: $(\rho_R/\rho_F)_{ACID} = 3.9$. Yet for the activation barriers the polar effects were dominant: $(\rho_R/\rho_F)^{\ddagger} = 0.26$. Subsequently, Bernasconi and Wenzel employed a three-parameter treatment to correlate six examples of $Y{-}CH_3$ adding polarizability (σ_α) to the original two effects.[11d] The outcome (using MP2/6-311+G** results) was qualitatively similar with ratios of 4.5 and 0.43, respectively. Polarizability constituted only 2% of the effect on equilibrium acidity but 19% on the rates. The important conclusions were that the anion products are strongly stabilized by resonance (where structurally possible), with significant but smaller stabilization by the field effect, and perhaps some destabilization through polarizability (although the effect is very small). On the other hand, although resonance stabilizes the transition states, the field effect is enhanced in the ts relative to the anion. Polarizability is stabilizing and is more important in these transition states than in the anions according to Bernasconi and Wenzel because its influence is reduced whenever the Y group carries a large amount of negative charge, as in the anionic state. For a more complete discussion of these results, see their paper.

(39) Dewar, M. J. S.; Zoebisch, E. G.; Healy, E. F.; Stewart, J. J. P. *J. Am. Chem. Soc.* **1985**, *107*, 3902.
(40) Hansch, C.; Leo, A.; Taft, R. W. *Chem. Rev.* **1991**, *91*, 165.

Table 7. Gas-Phase Substituent Constants[a] and Calculated Reaction and Activation Enthalpies[b] (kcal/mol) for Deprotonation at Saturated Carbon (MP2/6-311+G**)

system	σ_F	σ_{R^-}	σ_a	ΔH_{ACID}	ΔH_{CX}	$\Delta H^{\ddagger}$
2. $HC{\equiv}CCH_2\mathbf{H}$	0.23	0.15	−0.60	385.4	−8.5	0.4
4. $H_2C{=}CHCH_2\mathbf{H}$	0.06	0.16	−0.50	389.5	−6.5	3.0
6. $CH_3CH_2CH_2\mathbf{H}$	0	0.02	−0.49	415.2	−3.9	4.5
8. $O_2NCH_2\mathbf{H}$	0.65	0.18	−0.26	360.1	NA[c]	−8.44
9. $O_2NCH\mathbf{H}CH_3$[c]	0.65	0.21	−0.61	359.8	NA[c]	−9.8
10. $O_2NC\mathbf{H}(CH_3)_2$[d]	0.65	0.24	−0.96	360.7	NA[c]	−11.8
11. $O{=}NCH_2\mathbf{H}$[e]	0.41	0.26	−0.25	352.3	NA[c]	−1.45
12. $F_3CCH_2\mathbf{H}$	0.44	0.07	−0.25	384.0	−11.4	−4.5
13. $O{=}CHCH_2\mathbf{H}$	0.31	0.19	−0.46	367.5	NA[c]	−1.8
14. $N{\equiv}CCH_2\mathbf{H}$	0.60	0.10	−0.46	374.5	−14.2	−9.0
15. $CH_3SO_2CH_2\mathbf{H}$	0.59	0.12	−0.62	367.5	NA[c]	−10.7

[a] Taken from: Hansch, C.; Leo, A.; Taft, R. W. *Chem. Rev.* **1991**, *91*, 165. See also: Taft, R. W.; Topsom, R. D. *Prog. Phys. Org. Chem.* **1987**, *16*, 1. [b] ΔH_{ACID}, ΔH_{CX}, and $\Delta H^{\ddagger}$ values listed here were obtained using HF/6-311G** zero-point vibrational energies. [c] These complexes are not $C{-}H{\cdots}C^-$ complexes; see text. [d] These values are the sums of those for the nitro group and the methyl group(s). [e] Calculated from data of: Bernasconi, C. F.; Wenzel, P. J. *J. Org. Chem.* **2001**, *66*, 968.

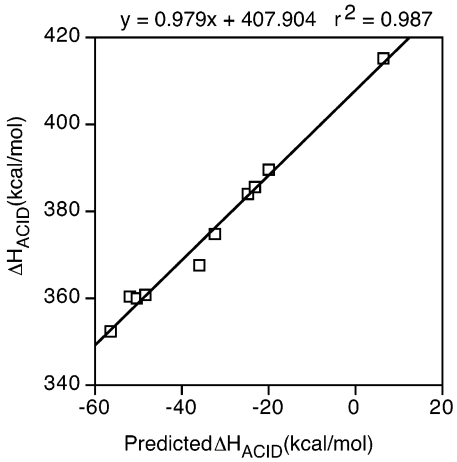

Figure 5. Plot of predicted ΔH_{ACID} values using gas-phase polar, resonance, and polarizability substituent constants versus MP2/6-311+G** ΔH_{ACID} values. See eq 5.

We report here a three-parameter treatment of our results for 11 acids, Y−C−H, entries 2, 4, 6, 8−15 in Tables 1 and 3. The relevant parameters are listed in Table 7. The results provide the following excellent correlations for ΔH_{ACID} and $\Delta H^{\ddagger}$, shown also in Figures 5 and 6.

$$\Delta H_{ACID} = -40.2\sigma_F - 143.2\sigma_R - 20.2\sigma_\alpha + 408.8 \quad r^2 = 0.987\ (n = 10) \quad (5)$$

$$\Delta H^{\ddagger} = -23.6\sigma_F + 9.7\sigma_R + 5.7\sigma_\alpha + 6.7 \quad r^2 = 0.992\ (n = 11) \quad (6)$$

Inclusion of the ΔH_{ACID} value for dimethyl sulfone led to a large difference between the computed value and that projected from the three-parameter fit; it is therefore not included in eq 5. The computed $\Delta H^{\ddagger}$ value for this compound did, however, agree well with that predicted from eq 6. Moreover, the computed and experimental ΔH_{ACID} values are in good agreement; see Table 1. Therefore, we suspect that one or more of the substituent constants for the CH_3SO_2 group is not performing well. Correlation (6) includes all 11 points and is dominated by the polar effect, whereas correlation (5), in which the resonance and polarizability effects are much more important

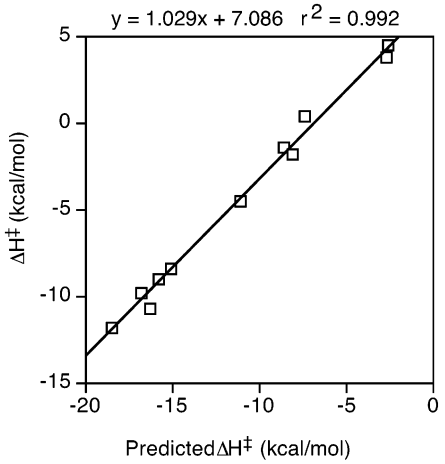

Figure 6. Plot of predicted $\Delta H^{\ddagger}$ values using gas-phase polar, resonance, and polarizability substituent constants versus MP2/6-311+G** $\Delta H^{\ddagger}$ values. See eq 6.

for dimethyl sulfone, does not accommodate that entry. Thus, the σ_R or the σ_α value for the CH_3SO_2 group is implicated as the troublesome substituent constant.

The outcomes are in general accord with the previous results. In discussing structural effects, we must first note a distinction between the two processes under consideration. ΔH_{ACID} measures formation of an anion and a separated proton from a neutral species of virtually the same size and composition as the anion. $\Delta H^{\ddagger}$ measures formation of a symmetrical, bimolecular entity from separated reactants, an anion and its neutral conjugate acid.

Resonance effects dominate in anion formation with those anions best able to delocalize charge (those with the largest σ_R values) profiting greatly from this effect. Yet polar effects can also be significant, especially for groups with large σ_F but small σ_R values. The anion-destabilizing influence of polarizability is relatively small, but is significant for substituents with large σ_α values but small σ_F and σ_R constants.

Polar and polarizability effects influence $\Delta H^{\ddagger}$ because intermoiety interactions exist in the transition state which have no counterpart in the separated reactants. Polar effects dominate with the resonance effect actually destabilizing the ts relative to the anion. This is sensible because resonance stabilization, fully expressed in the anion, is partly lost at the transition state. If these symmetrical transition states were perfectly balanced with respect to loss of resonance stabilization on the part of the anionic reactant and gain of same in the formerly neutral reactant, then the net resonance effect on $\Delta H^{\ddagger}$ would be zero. The fact that it is not is a direct indicator of transition state imbalance. The polarizability effect is stabilizing in the transition state.[41] Among other consequences, this allows the addition of methyl groups in the series, nitromethane, nitroethane, 2-nitropropane, to *lower* the activation barrier in the gas phase, a result in direct contrast to the order in aqueous solution. We therefore affirm that there is no nitroalkane anomaly in the gas phase even though there is transition state imbalance.

Substituent effects on anion−molecule complex formation have not been analyzed previously in this way. The solutions resulting from our attempted three-parameter fit were not stable because of a deficiency of data points. However, they indicate qualititatively that polar effects are the dominant interaction between the anion and the neutral in the complex. The apparent absence of important contributions from resonance and polarizability effects in complex formation can be traced to the fact that the interaction occurs without substantial changes in bond order and at relatively long range. A look at the signs of the ρ values in the activation energy correlation shows that, in this case, resonance and polarizability tend to offset each other.[41] Thus, polar effects in the ts greatly outweigh the combined effects of resonance and polarizability, permitting the excellent correlation noted earlier between ΔH_{CX} and $\Delta H^{\ddagger}$.

We have also attempted a dual parameter correlation involving the same set of C−H acids using our COSMO solvation model results for ΔH_{ACID}, ΔH_{CX}, and $\Delta H^{\ddagger}$. For the polar substituent constants, we used the gas-phase σ_F constants as these are almost identical to Taft's σ_I constants.[40] For resonance effects, the proper choice is not obvious. We have chosen to use ($\sigma_p^- - \sigma_p$), the difference between σ^- constants for *para* substituents and σ_p, the standard Hammett constant for *para* substituents. This difference should isolate the resonance component of the σ^- values from the polar part. We did not include a set of polarizability constants. In any case, the measures of fit are not nearly as good as with the gas-phase results, and we can make only a qualitative statement. The relative importance of polar and resonance effects on ΔH_{ACID} favors resonance, but not by much. For ΔH_{CX} and for $\Delta H^{\ddagger}$, polar effects are dominant. These trends are qualitatively the same as for the gas-phase computations, but uncertainties regarding the suitability of the computational model and of the appropriate substituent constants allow no more to be inferred.

It is relevant here to recall that a dual substituent parameter treatment has also been applied to the rates and equilibria of the deprotonation of a series of *p*-substituted arylnitromethanes in DMSO solution, eq 7.[22a] In this medium, the pK_a values are sensitive both to polar (σ_I) and to resonance effects with a ratio of (ρ_R/ρ_I) = 0.87. The activation barriers, however, are

$$Ar{-}CH_2{-}NO_2 + PhCO_2^- \rightarrow PhCO_2H + Ar{-}CH{-}NO_2^- \quad (7)$$

substantially more sensitive to polar effects: (ρ_R/ρ_I) = 0.47. The difference in the two ratios is in qualitative agreement with the relative importance of polar and resonance effects described just above for the gas phase and suggest that transition state imbalances in the gas and solution phases have some sources in common. The increased sensitivity to resonance effects of the equilibrium acidities in the gas phase ($\rho_R/\rho_F = 4.3$) reflects the increased need for charge dispersal in the anionic conjugate base when there is no dielectric medium to interact with the charge.

Performance of the COSMO Solvent Model. We are interested in determining how well the aqueous solvent model used in this study reflects known aqueous phase results. First, recall that geometries were not optimized with COSMO; gas-phase MP2 optimized geometries were used instead. This fact introduces an uncertainty of unknown magnitude. However, taking our results at face value, we could apply four criteria to the performance of the model: the ability of the model to reproduce experimental solution-phase results; the qualitative nature of the reaction energy surfaces; comparison of transition

(41) Because σ_α values are negative,[40] a negative ρ value results in $\rho\sigma_\alpha > 0$, which raises the barrier.

state imbalance parameters with those calculated for the gas phase; and prediction of the nitroalkane anomaly.

As discussed above, COSMO ΔH_{ACID} values correlate well with aqueous pK_a values. The fit is not as good as the gas-phase correlations, but it is better than the correlations between COSMO results and gas-phase results, both experimental and computed; see Table 2.

The reaction energy profiles calculated by COSMO show that the anion−molecule complexes lie above the reactant state and below the transition state, just as expected for solution and in contrast to the gas phase wherein complexation is exothermic.

The TSIP values calculated from COSMO atom and group charges vary little from those calculated using the gas-phase methods. As described in the Introduction and mentioned again in the Transition State Imbalance section, there is reason to expect that these values should be larger in solution, particularly in H-bonding donor solvents.

A partial nitroalkane anomaly does emerge from COSMO calculations. In water, the acidity order of the simple nitroalkanes is 2-nitropropane > nitroethane > nitromethane. In the gas phase, the experimental ΔH_{ACID} values are within experimental error, while computationally the order is nitroethane > nitromethane > 2-nitropropane for all methods, including COSMO. However, the COSMO activation barriers for the identity reactions in this series are in the order nitromethane < nitroethane < 2-nitropropane, just as in water, and opposite from the computed gas-phase order. Thus, whereas COSMO does not recreate the aqueous acidity order, it does reproduce the kinetic reactivity order.

As mentioned above, the COSMO model uses a dielectric continuum environment rather than employing specific molecular interactions between solutes and the medium. Apparently it is this deficiency which prevents the model from accurately reproducing small differences in ΔH values which are attributable to strong, specific intermolecular interactions such as H-bonding to the oxygen atoms of the nitroalkane anions. To test this point, we carried out MP2/6-311+G** calculations on "microhydrated" nitroalkane anions, eq 8.

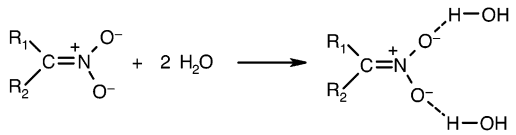

(8)

R_1R_2 = H, H	ΔH_{HYD} = -30.1 kcal/mol
R_1R_2 = H, CH_3	ΔH_{HYD} = -30.7 kcal/mol
R_1R_2 = CH_3, CH_3	ΔH_{HYD} = -31.4 kcal/mol

The resulting ΔH_{HYD} values show that, indeed, hydrogen bonding stabilizes the anions such that the acidity order tends toward that in water. (We assume that differential solvation effects on the neutral nitroalkanes are relatively insignificant.) Concomitantly there occur predictable geometric changes within the anion moieties of the microhydrated species: The C═N bonds are shorter than those in the gas phase by 0.013−0.015 Å, while the N−O bonds lengthen by 0.006−0.011 Å. These changes reflect "solvent-enhanced" relocation of the negative charge away from carbon and toward the oxygens.

Conclusions

A number of general or specific points come from this work. These include: (1) Transition states for gas-phase proton-transfer reactions are stabilized by an important contribution from triple-ion character, represented by structure **2b** ($Y-X^- H^+ {}^-X-Y$). The importance of this contribution and of its stabilizing effect is greater as reaction terminus X is more electronegative. This result supports conclusions reached in earlier work.[24] We postulate that the same generalization holds for proton transfers in solution. Also critical is the extent of π delocalization into each group Y allowed by geometrical constraints and by the amount of charge transferred from the base and therefore available for delocalization.[16b] In identity reactions, this amount is one-half the difference between the total charge, −1, and the positive charge on the proton in flight. The charge on the proton in flight is greatest for proton transfers between the most electronegative X atoms; hence moiety Y−X has the greatest negativity in those cases. A relatively small fraction of this is delocalized, enhancing the importance of structure **2b**.

(2) Anion−molecule complexation energies correlate very well with activation energies for identity proton-transfer reactions. A smaller number of nonidentity reactions also fit the correlation well. We conclude that the forces which stabilize the complex, especially electrostatic or H-bonding forces, are also of major importance in the ts. This statement is buttressed by the fact that a multiple substituent parameter treatment of the data shows that both ΔH_{CX} and $\Delta H^{\ddagger}$ are predominantly determined by polar effects, in part because resonance and polarizability effects tend to offset one another in the ts.

(3) Correlation between computed ΔH_{ACID} and $\Delta H^{\ddagger}$ values is poor, except for carefully selected, small subsets of data. We attribute this failure to the fact that many interactions within the ts arise from its bimolecular nature and are irrelevant to the separated reactants and products.

(4) Comparative transition state imbalance parameters (TSIPs) can be useful indicators of transition state imbalance in a set of identity proton-transfer reactions, but only if the atom (X) between which the proton is transferred is not varied within the set. The more electronegative is atom X, the greater will be the calculated TSIP, other factors being similar. This is because such atoms retain much of the negative charge in the ts so that electrostatic interactions within $[X^{\delta-}\cdots H^{\delta+}\cdots X^{\delta-}]^{\ddagger}$ can be optimal.

(5) Computed ΔH_{ACID} and $\Delta H^{\ddagger}$ values for a set of arylnitromethanes as well as for the series, nitromethane, nitroethane and 2-nitropropane, indicate that the nitroalkane anomaly is not manifest in the gas phase.

(6) The CPCM-B3LYP/6-311++G** (COSMO) aqueous solvent model provides ΔH_{ACID} values which correlate well with experimental aqueous pK_a values. A similar result has been obtained previously.[9k] The computed results for the set nitromethane, nitroethane, and 2-nitropropane can be compared with experimental aqueous phase results. Within this very limited set, the computed and experimental acidity orders do not agree. However, COSMO does give the same order, qualitatively, for the activation barriers in this set and therefore partially reproduces the nitroalkane anomaly. The model also correctly gives endothermic complexation energies and still more endothermic activation energies. It does not, as we had expected, lead to larger TSIP values. An attempt to carry out a multiple parameter substituent effect correlation gave much poorer fits than for the gas-phase correlations; a number of uncertainties render any conclusions highly tentative. Not surprisingly, the

performance of this solvation model for the present purposes is compromised when strong, specific solute−solvent interactions such as hydrogen bonding make critical contributions. For such cases, a hybrid approach using microsolvated solute species within the COSMO model might lead to better agreement with experiment.

Acknowledgment. Part of this work was carried out at Lawrence Livermore National Laboratory under contract W-7405-ENG-48 from the U.S. Department of Energy. The authors thank the DOE Undergraduate Research Semester Program for support. The support of the National Science Foundation (CHE-9974506) is gratefully acknowledged by S.G.

Supporting Information Available: Tables S1 (energies), S2 (group charges), and S3 (transition state imbalance components) (PDF). This material is available free of charge via the Internet at http://pubs.acs.org.

JA0356683